GLUTATHIONE TRANSFERASE Z1-CATALYZED BIOTRANSFORMATION OF DICHLOROACETATE – ROLES OF MITOCHONDRION, SUBJECT AGE, GSTZ1 HAPLOTYPE AND CHLORIDE INTERACTION

By

WENJUN LI

A DISSERTATION PRESENTED TO THE GRADUATE SCHOOL
OF THE UNIVERSITY OF FLORIDA IN PARTIAL FULFILLMENT
OF THE REQUIREMENTS FOR THE DEGREE OF
DOCTOR OF PHILOSOPHY

UNIVERSITY OF FLORIDA

2011

To my mom and dad,
and those who have loved and supported me

ACKNOWLEDGMENTS

Five years of graduate school have helped me mature as a researcher and as an individual. First and foremost, I would like to deliver my most sincere thanks to Dr. Margaret James, my Ph.D. mentor and role model during these years. I deeply appreciate the continuous support, encouragement and enlightenment Dr. James has provided throughout my Ph.D. study. Her dedication, fairness and integrity to work and her kindness and respect to people have and will always guide me in my own research and doings.

My gratitude extends to my collaborators and committee members. Dr. Peter Stacpoole has provided me with expert insights into dichloroacetate research and firsthand information from clinical studies, both of which motivated me to dig deeper into the study and reminded me of our goal of helping people. Drs. Ronald Hines and Taimour Langaee have both given me generous assistance in various aspects of the study. I am thankful to Drs. Ken Sloan, Raymond Booth and Raymond Bergeron for assisting with the dissertation and their support during graduate study.

I would like to thank all of my fellow students and colleagues for their support and encouragements. In particular, Yuan Gu has made substantial contributions to our study and Sriram Ambadapadi has been so kind to hold our regular coffee breaks. Special thanks goes to my fiancé Zhuming Sun, who truly knows me and cares for me. Together, we walk through the happiness and bitterness of research and life. Finally, I am most grateful to my parents for their forever love, support and understandings. They are friends and teachers of my life.

TABLE OF CONTENTS

page

LIST OF TABLES

LIST OF FIGURES

LIST OF ABBREVIATIONS

δ-ALA	delta-aminolevulinate
ALDH1A1	aldehyde dehydrogenase 1A1
AUC	area under plasma concentration-time curve
CypD	Cyclophilin D
CytC	Cytochrome *C*
DCA	dichloroacetate
DME	drug metabolizing enzyme
ESI-QTOF	electrospray ionization hybrid quadrupole time of flight
FA	fumarylacetone
FAA	fumarylacetoacetate
GSH	glutathione
GSTZ1	glutathione transferase zeta 1
HPLC	high-performance liquid chromatography
IM	inner membrane
IMS	intermembrane space
LOD	limit of detection
MA	maleylacetone
MAA	maleylacetoacetate
MAAI	maleylacetoacetate isomerase
MCA	monochloroacetate
MELAS	mitochondrial myopathy, encephalopathy, lactic acidosis and stroke-like episodes
MWCO	molecular weight cutoff
OM	outer membrane
PDC	pyruvate dehydrogenase complex

S-D	Sprague-Dawley
SNP	single nucleotide polymorphism
$t_{1/2}$	elimination half-life

Abstract of Dissertation Presented to the Graduate School
of the University of Florida in Partial Fulfillment of the
Requirements for the Degree of Doctor of Philosophy

GLUTATHIONE TRANSFERASE Z1-CATALYZED BIOTRANSFORMATION OF DICHLOROACETATE – ROLES OF MITOCHONDRION, SUBJECT AGE, GSTZ1 HAPLOTYPE AND CHLORIDE INTERACTION

By

Wenjun Li

May 2011

Chair: Margaret O. James
Major: Pharmaceutical Sciences – Medicinal Chemistry and Toxicology

Dichloroacetate (DCA) is a potential environmental hazard and an investigational drug. By inhibiting pyruvate dehydrogenase kinase in the mitochondria, DCA remodels cellular energy metabolism and therefore is studied for treatments of lactic acidosis and, recently, solid tumors. DCA inactivates its own metabolizing enzyme glutathione transferase Z1 (GSTZ1). Thus, repeated doses of DCA result in reduced drug clearance, an effect shown to be influenced by subject age and GSTZ1 haplotype. In this study, we investigate the roles of mitochondrion, subject age, GSTZ1 haplotype and chloride ion on GSTZ1-catalyzed biotransformation of DCA in human liver.

We demonstrated that mitochondrion is a novel site of DCA biotransformation catalyzed by GSTZ1, an enzyme co-localized in cytosol and mitochondrial matrix. GSTZ1 activity with DCA was 2.5 – 3-fold higher in cytosol than in whole mitochondria, being proportional to its protein content in the two compartments. Rat mitochondrial GSTZ1 had a 2.5-fold higher $^{App}K_m$ for glutathione than cytosolic GSTZ1, whereas the $^{App}K_m$s for DCA were identical. DCA treatment at 500 mg/kg/day for 8 weeks inactivated liver mitochondrial and cytosolic GSTZ1 to a similar extent (~10% of control) in rats.

By studying human liver cytosols from 10 weeks of gestation to 74 years of life, we demonstrated age as the major determinant of GSTZ1 protein expression and activity with DCA during human liver development. With very low levels in the fetus, GSTZ1 expression and activity increased in the neonatal period, rose further over the course of children development and attained variable but similar levels between ages 7 and 74. GSTZ1 haplotype showed no effect on protein expression but affected enzyme activity with DCA. Z1A carriers, in general, possessed a ~3-fold higher activity with DCA than noncarriers at a given level of expression.

Chloride, a major electrolyte in the body, was shown by the current study to protect GSTZ1 from DCA inactivation in a Cl^- concentration- and GSTZ1 haplotype-dependent manner. To achieve 50% protection of cytosolic GSTZ1 in a 2 h incubation with 0.5 mM DCA, 33.6 mM Cl^- was required for Z1C/Z1A subjects compared to ~13 mM for Z1C and Z1D homozygous subjects. At physiological concentration of chloride (38 mM), the inactivation half-life of GSTZ1 was 2-fold longer in Z1C and Z1D homozygous subjects (over 5 h) than Z1C/Z1A subjects (2.5 h).

CHAPTER 1
INTRODUCTION

DCA as an Environmental Agent

Dichloroacetate (DCA) is a ubiquitous molecule in our biosphere. Human populations can be exposed to DCA through consumption of chlorinated drinking water and food, bathing or swimming in chlorinated pools, or in vivo metabolism of certain xenobiotics and drugs. DCA is generated as a byproduct during water chlorination, and, is detected in U.S. municipal water supplies at concentrations of 30 – 160 μg/L (Mughal, 1992). People are estimated to be exposed to a few μg DCA / kg body weight daily by drinking municipal water. DCA is also detected in swimming pool water and some raw and processed foods (WHO, 2005); it can be formed during the in vivo metabolism of certain pharmaceuticals, such as chloral hydrate (Henderson et al., 1997), as well as widely used industrial solvents, trichloroethylene and perchloroethylene (Monster, 1986), both of which may be released into the atmosphere and contaminate surface water. However, as the rate and extent of DCA absorption via these routes have not been determined, their contribution to DCA environmental exposure level remains unclear.

To an environmental toxicologist, DCA is considered to be an environmental carcinogen based on its ability to induce liver tumors in inbred strains of rodents at doses hundreds to thousands of times higher than levels encountered through the environment (Bull, 2000). Several mechanisms have been postulated for the carcinogenic effect of DCA: peroxisome proliferation, hypomethylation and mutagenicity of DNA, glycogen accumulation, and reparative hyperplasia following injury (Bull, 2000; WHO, 2004). However, the relevance of these findings in rodents to humans is lacking.

So far, no evidence of DCA causing neoplasia in humans has been reported. The potential health risks of DCA at environmental levels have been recently reviewed and data do not support DCA to be a hazard to general populations at large (Stacpoole, 2011).

DCA as a Therapeutic Agent

As a therapeutic agent, DCA was first synthesized as an ion complex with diisopropylammonium in 1952 by Krebs and Krebs during the exploration of Vitamin B15 (pangamic acid) (Stacpoole, 1969). Since then the pharmacological effects of DCA have been extensively studied and the therapeutic and investigational uses of DCA keep expanding. Administered as the diisopropylammonium salt during the 60s and as the sodium salt later on, DCA has been used clinically over 50 years for the treatment of several metabolic and cardiovascular disorders, including diabetes mellitus, hyperlipoproteinemia, and lactic acidosis (Stacpoole, 1989). Recently, DCA was studied in several clinical trials for chronic treatment of genetic mitochondrial diseases, such as congenital lactic acidosis, pyruvate dehydrogenase complex (PDC) deficiency, and mitochondrial myopathy, encephalopathy, lactic acidosis and stroke-like episodes (MELAS) (Barshop et al., 2004; Berendzen et al., 2006; Kaufmann et al., 2006; Stacpoole et al., 2006; Stacpoole et al., 2008). As a metabolic modulator, DCA is currently being investigated for anti-proliferative and pro-apoptotic effects in pulmonary arterial hypertension and cancer (McMurtry et al., 2004; Michelakis et al., 2008).

The rationale for DCA therapy is based on its ability to efficiently stimulate the activity of pyruvate dehydrogenase complex (PDC). PDC is a multi-enzyme complex that catalyzes the irreversible oxidation of pyruvate to acetyl coenzyme A (CoA) (Figure 1-1). Pyruvate is a pivotal molecule in the cellular carbon fuel and energy metabolism.

Produced from glucose by glycolysis in the cytosol, pyruvate is converted to lactate and alanine in cytosol, or is transported into mitochondria and oxidized to acetyl CoA. Under aerobic conditions, this equilibrium is determined by the activity of PDC, which is in turn regulated by reversible phosphorylation. PDC is phosphorylated to the inactive state by PDC kinase and dephosphorylated to the active state by PDC phosphatase. DCA inhibits PDC kinase, thus “locking” PDC in its unphosphorylated and catalytically active state, and increasing the oxidation of pyruvate to acetyl CoA. As a result, DCA promotes the flux of pyruvate into mitochondria to enter the Krebs cycle, and simultaneously reduces the amount of alanine and lactate in the cytosol. Because reducing equivalents of NADH and $FADH_2$ are generated during PDC-catalyzed reaction and Krebs cycle, the respiratory chain is in turn stimulated to generate reactive oxygen species and ATP. Such effects on restoring mitochondrial energy production and thus overcoming the Warburg effect contribute to the emerging roles of DCA as a metabolic modulator in cancer and pulmonary arterial hypertension (Archer et al., 2008; Michelakis et al., 2008).

For therapeutic uses, sodium DCA is administered at 10 mg/kg to over 100 mg/kg intravenously or by mouth for a few days to over several years. Patients treated with DCA are reported to develop occasional asymptomatic hepatotoxicity and more frequently a peripheral neuropathy. The reversible peripheral sensory-motor neuropathy is the major adverse effect that limits chronic DCA use, and, occurs more frequently in adults than children (Kaufmann et al., 2006; Stacpoole et al., 2006; Stacpoole et al., 2008). Clinical manifestations include tingling of the fingers and toes and weakness of

the facial and distal muscles of the extremities; however, the mechanism of this toxicity is still under investigation.

DCA Biotransformation

GSTZ1 as the Metabolizing Enzyme

The initial step of DCA biotransformation is the dechlorination to glyoxylate. This reaction is glutathione (GSH)-dependent and catalyzed exclusively by glutathione transferase zeta 1 (GSTZ1), a member of the GST superfamily.

GST superfamily consists of two distinct and structurally unrelated groups: the soluble GSTs and the microsomal and membrane-bound GSTs. GSTZ1 belongs to the soluble GSTs, which constitute up to ~10% of cellular protein and is a major family in Phase II drug metabolizing enzymes (DMEs). To date, seven classes of soluble GSTs have been identified in mammals, namely GST Alpha, Mu, Pi, Theta, Zeta, Omega and Sigma (Mannervik et al., 2005). Liver cytosol is the principal location for the soluble GSTs. Recently, several members of soluble GSTs, e.g. GST A4, P1, M1 and O1, were also found to be present in mitochondria and/or nucleus (Hayes et al., 2005; Gallagher et al., 2006; Goto et al., 2009). Like other soluble GSTs, GSTZ1 is present in the cytosol and expressed most abundantly in the liver (Lantum et al., 2002a).

GSTs are dimeric proteins in nature. Both homodimers and heterodimers of different subunits within the same class have been observed in tissue. So far, only one subunit of the zeta class, i.e. Z1, has been identified in mammalian species. Accordingly, only the homodimeric form of this protein, i.e. GST Z1-1, is known (Board et al., 1997; Polekhina et al., 2001). For convenience, we use GSTZ1, which in essence refers to its homodimer, in the remainder of the document.

Members of GSTs catalyze a variety of reactions, including conjugation, addition-elimination and isomerism. These reactions are dependent on GSH, the cofactor of GSTs. Common substrates, such as 1-chloro-2,4-dinitrobenzene and ethacrynic acid, exist for GSTs. However, GSTZ1 has little or no activity with these prototypical substrates (Board et al., 1997). Instead, it catalyzes the dehalogenation of α-halo carboxylic acids (Tong et al., 1998a). For example, GSTZ1 converts dichloroacetate and chlorofluoroacetate to glyoxylate (Figure 1-2A). This difference in substrate selectivity can be explained, in part, by the structural features of GSTZ1 active site. Revealed by the crystal structure, the hGSTZ1 active site is a lot smaller and composed of more polar residues than other GSTs, which may contribute to its preference for relatively small and polar substrates, such as short chain α-halo acids (Polekhina et al., 2001).

Identified by the bioinformatics approaches in the late 90s, GSTZ1 is proven identical to the long known maleylacetoacetate isomerase (MAAI) (Blackburn et al., 1998; Fernandez-Canon and Penalva, 1998). It isomerizes maleylacetoacetate (MAA) and its analog maleylacetone (MA) respectively to fumarylacetoacetate (FAA) and fumarylacetone (FA) at the penultimate step of tyrosine/phenylalanine catabolism (Figure 1-2B). Human recombinant GSTZ1 possesses hundreds to thousands-fold higher specific activities for the endobiotic substrate MA than for DCA and other xenobiotic substrates (Table 1-1) (Board and Anders, 2005). Species differences in DCA biotranformation are observed in that V_{max}/K_m for mouse liver cytosol was 1.6-fold and 6.4-fold higher than those for rat and human, respectively (Tong et al., 1998a).

DCA-Induced Inactivation of GSTZ1

In vivo studies of DCA in rats demonstrate that DCA treatment reduces the protein expression and activity of liver cytosolic GSTZ1 in a dose- and duration-dependent manner (Anderson et al., 1999; Cornett et al., 1999). At lower doses (4 and 12.5 mg/kg/day), 5 days of treatment were required to reduce GSTZ1 activity to ~50-80% of control level. Whereas, 60% inhibition of GSTZ1 was achieved by a single dose of 50 mg/kg DCA and over 90% inhibition by 1000 mg/kg DCA (Cornett et al., 1999). Restoration of GSTZ1 activity occurred gradually over days to weeks after cessation of DCA treatment (Anderson et al., 1999; Guo et al., 2006). In all cases, changes in GSTZ1 activity are positively correlated to its protein expression without affecting mRNA level (Anderson et al., 1999; Ammini et al., 2003; Guo et al., 2006).

Studies from Anders' lab (Tzeng et al., 2000) demonstrated time- and DCA concentration-dependent inactivation of GSTZ1 in vitro using recombinant enzymes and liver cytosols from human, rat and mouse. The reaction required GSH and could not be reversed by dialysis. The same lab reported a GSTZ1 protein adduct formed between the active site residue Cys16 and a proposed metabolic intermediate of DCA (Anderson et al., 2002). This adducted GSTZ1 was suggested to be inactive and undergo rapid proteolysis in vivo based on the observed parallel decreases in protein activity and immunoreactivity after DCA administration (Anderson et al., 1999). Together with the unaffected level of mRNA, DCA-induced inactivation of GSTZ1 appeared to be wholly a post-transcriptional event, probably through covalent modification of GSTZ1 followed by rapid degradation.

Discrepancy in studies of GSTZ1 inactivation

The inactivation half-life of human liver cytosolic GSTZ1 was reported to be 22 min by incubating with 0.5 mM DCA and 5 mM GSH in potassium phosphate buffer (Tzeng et al., 2000). In stark contrast, a previous study from our lab found no loss of GSTZ1 activity at all in human liver cytosol after 30 min incubation with the same concentration of DCA and 1 mM GSH in Hepes buffer (Cornett et al., 1999). Careful examination of the assay conditions revealed the presence of chloride ion in our protein samples but not in Tzeng's, which was caused by the difference in dialysis buffer compositions.

Chloride is a major electrolyte in the human body. It is present at ~100 mM in the serum and ~38 mM in the liver for adults under normal physiological condition (Widdowson and Dickerson, 1960; Morrison, 1990). Defects in chloride homeostasis are implicated in a number of diseases, including but not limited to cystic fibrosis, kidney dysfunctions and neurological disorders (De Koninck, 2007; Edwards and Kahl, 2010). Thus, literature has largely been focused on the flux of chloride across membranes and cellular events triggered following the flux, with regard to chloride function (Edwards and Kahl, 2010). In addition, chloride modulation of protein function has been documented. These include both positive and negative effects on enzyme activity (Garcia-Espana et al., 1991; Meijer et al., 1992), drug-receptor interaction (Tavoulari et al., 2009) and protein oligomerization (Kitani and Fujisawa, 1984; Sasaki et al., 2009).

GSTZ1 Polymorphism

Genetic polymorphism of DMEs is well recognized as a major contributor to the inter-individual differences in drug response. Non-synonymous single nucleotide polymorphisms (SNPs) can occur in the coding or regulatory region of a gene and thus result in an altered function and/or expression of the gene product (protein). Several

classes of GST enzymes, e.g. A, M, T and P, are encoded by genes with functional polymorphisms. Most notably, individuals carrying null alleles of GST M1 and T1 have been suggested to be associated with an increased risk of certain cancers and some adverse health outcomes (Hayes et al., 2005). For example, a recent meta-analysis of GST polymorphism and colorectal cancer risk showed an increased risk in GSTM1 and GSTT1 null allele carriers in Caucasian populations (Economopoulos and Sergentanis, 2010).

To date, five non-synonymous SNPs have been reported in the coding region of human *GSTZ1* gene. These include four SNPs (T23C, Leu8Pro; G94A, Glu32Lys; G124A, Gly42Arg; and C245T, Thr82Met) identified through analysis of expressed sequence tag database (Blackburn et al., 2000; Blackburn et al., 2001) and one newly discovered SNP (G295A, Val99Met) during human DCA pharmacokinetic study (Shroads et al., 2011). Except for L8P, GSTZ1 haplotypes bearing other SNPs have been found in populations with varying frequency: EGT (Z1C) is the most common variant (~50%), followed by KGT (Z1B) (~30%) and EGM (Z1D) (~15%), while KRT (Z1A) (~5%) and KGM (0.4%) are the rarest. The V99M variant was identified just recently in one individual bearing EGM, however, its occurrence in populations has not been studied.

The recombinant proteins of the four common GSTZ1 variants, EGT, KGT, EGM and KRT, exhibit different catalytic activities with a range of substrates (Board and Anders, 2005) (Table 1-1). The wild type EGT allele had the highest activity with endogenous substrate MA, followed by KGT while KRT and EGM had 80% lower activities. With chlorofluoroacetate, similar activities were observed among variants.

Nevertheless, the less frequently occurring variant KRT had 4-5-fold higher specific activity with DCA as substrate than the other three variants, for which the activities were similar. Interestingly, different rates in DCA inactivation were also observed between variants in that the inactivation half-life was twice as long with KRT as the others. Thus, it was postulated that the higher specific activity of KRT for DCA may due to its slower rate of inactivation (Tzeng et al., 2000).

Polymorphisms in the regulatory region, which may modulate gene transcription and expression, have been shown to contribute to the inter-individual variations in drug response (Hines et al., 2008). Fang et al. (2006) identified 10 SNPs in the promoter region of GSTZ1 from a sampled population but found no significant regulatory effects.

DCA Pharmacokinetics

Overview of DCA Absorption, Distribution, Metabolism and Elimination

A typical therapeutic dose range of DCA in humans is 25-100 mg/kg/day for short-term and chronic treatment (Stacpoole et al., 1998). Due to its high affinity for the monocarboxylate transport system that facilitates cellular uptake, DCA is quickly absorbed after oral administration and has a bioavailability approaching unity at therapeutic doses (Stacpoole et al., 1998). Stimulation of PDC activity generally occurs minutes after oral or parenteral DCA administration, and DCA peak plasma level is reached within 30 min p.o. (Stacpoole et al., 2003). Consistent with mitochondria being the site of action, DCA is a substrate for mitochondrial pyruvate transporter so that it competes with pyruvate for entry into mitochondria (Figure 1-1).

Muscle and liver appear to be the major tissues of DCA distribution (James et al., 1998; Stacpoole et al., 1998). One hour after a single oral dose of 50 mg/kg ^{14}C-DCA to overnight fasted S-D rats, muscle and liver accumulated 22.5% and 16.3% of the dose,

respectively, followed by gastrointestinal tract (9.26%), fat tissue (4.58%), and kidney (1.37%). After dosing for 24 h, radioactivity decreased in all tissues, accompanied by marked increases of radioactivity in expired CO_2 (37.2%), urine (9.8%) and feces (1.39%) (James et al., 1998). The amount and distribution of DCA and its metabolites during excretion are shown to be dependent on the dosage and dosing schedule of DCA, as well as the species, age, and nutritional status of the subject. Nevertheless, CO_2 is the major metabolite identified in vivo, accounting for 19-44% of the DCA dose (Larson and Bull, 1992; Lin et al., 1993; James et al., 1998).

DCA undergoes extensive metabolism after oral and intravenous administration so that very little parent DCA is recovered in the urine after a single dose (Larson and Bull, 1992; James et al., 1998; Ammini et al., 2003; Guo et al., 2006). DCA is primarily dechlorinated to glyoxylate in the liver by GSTZ1 (Tong et al., 1998b). Glyoxylate can be further metabolized to glycine, glycine conjugates, oxalate, glycolate, and CO_2 by various enzymes in the cytosol and mitochondria (Figure 1-3). Less than 1% of a DCA dose can be reductively dechlorinated to the potential neuro-toxin, monochloroacetate (MCA) in the circulation through a not yet known mechanism (Shroads et al., 2008). Interestingly, the ratio of DCA reductive dechlorination to MCA did not increase in GSTZ1 knock-out mice even though the primary biotransformation pathway of DCA to glyoxylate was impaired (Ammini et al., 2003). Therefore, the alternative biotransformation of DCA to MCA probably has a minor role in the metabolism and toxicity of DCA.

Subject Age and GSTZ1 Genotype in Determining DCA Pharmacokinetics

After two decades of research on DCA pharmacokinetics, it is now well recognized that DCA inhibits its own metabolism and elimination by inactivating the metabolizing

enzyme GSTZ1. Therefore, DCA exhibits marked increases in area under plasma concentration-time curve (AUC) and elimination half-life ($t_{1/2}$) after just one or multiple prior doses, a phenomenon shown in humans regardless of gender, age, ethnicity, state of health, or route of administration (Curry et al., 1991).

Recently, subject age and GSTZ1 genotype emerged as important determinants of DCA pharmacokinetics. Study of chronic DCA treatment in children with heterogeneous causes of congenital lactic acidosis (mean age 5.2 years at entry, n = 5) and adults with MELAS (mean age 24 years at entry, n=4) revealed a striking age-dependent decrease in DCA plasma clearance. With the same dosing regime (12.5 mg/kg/12 h) and similar kinetic indices after first DCA dose, adults exhibited 10-fold increase in elimination $t_{1/2}$ and over 20-fold increase in AUC compared to the 3- and 4-fold increases, respectively, in children at the end of 6 months (Table 1-2). Treatment of S-D rats with 25 mg/kg/day DCA for 1 and 5 days reproduced similar age-related differences at DCA pharmacokinetics at day 5 (Shroads et al., 2008).

In addition to age, Shroads et al. (2011) recently reported the use of GSTZ1 haplotype as a criterion to segregate individuals to fast and slow DCA metabolizers. After 5 days of 25 mg/kg/day DCA, healthy adult subjects carrying at least one copy of EGT exhibited 3-fold faster plasma clearance than EGT non-carriers, especially those harboring G42R and/or T82M SNPs (Table 1-3). Similarly, EGT carriers in children with genetic mitochondrial diseases exhibit faster clearance of DCA than their EGT non-carrier counterparts after 12 months of treatment at 12.5 mg DCA/kg/12 h.

DCA Pharmacotoxicology

Postulated Mechanisms of DCA Toxicity

Reversible peripheral neuropathy is the major adverse effect in chronic DCA treatment. Although the mechanism is not yet elucidated, recent studies suggest that DCA-induced inactivation of GSTZ1/MAAI and subsequent disruption of phenylalanine/tyrosine catabolism may contribute to DCA toxicity.

Phenylalanine and tyrosine catabolic pathway is involved in several inborn errors of metabolism (Figure 1-4). Hereditary tyrosinemia type 1, caused by deficiency in the ultimate enzyme fumarylacetoacetate hydrolase, is the most severe form with symptoms of severe damage in hepatic, renal and nervous systems (Russo et al., 2001). The peripheral neuropathy that occurs both in patients with hereditary tyrosinemia type 1 and DCA treatment has been attributed in part to the elevated levels of neurotoxin delta-aminolevulinate (δ-ALA) and alkylating agents MAA and MA due to loss of functions of fumarylacetoacetate hydrolase or GSTZ1.

MAA and its decarboxylated product MA are known alkylating agents that can attack glutathione and other thiols (Lantum et al., 2002b). Cytotoxicity of MA was suggested to involve oxidative stress as shown in mouse hepatocytes and splenocytes (Lantum et al., 2003; Theodoratos et al., 2009). Additionally, accumulated MAA and FAA can be converted to succinylacetoacetate and succinylacetone. Succinylacetone is a potent inhibitor of δ-ALA dehydratase (Kic ~0.15 μM) that catalyzes the oxidation of δ-ALA to porphobilinogen during an early step in heme biosysnthesis. δ-ALA has been implicated as a neurotoxin in several neuropathies either through direct action as a pro-oxidant or subsequent perturbation of heme biosynthesis (Felitsyn et al., 2008). As a

result of succinylacetone action, the concentration of δ-ALA is increased in DCA and tyrosinemia patients, possibly contributing to the nerve toxicity.

Clinical Pharmacotoxicology of DCA

DCA-associated peripheral neuropathy occurs frequently in adult patients treated for genetic mitochondrial diseases, glioblastoma multiforme, and MELAS. Study of adult MELAS patients (mean age of entry was 30 years) with 12.5 mg DCA/kg/12 h ended prematurely due to significant worsening of drug associated neuropathy in some individuals after a few weeks of treatment (Kaufmann et al., 2006). In contrast, children (mean age of entry was 5.6 years) with heterogeneous causes of congenital lactic acidosis showed no worsening of hepatotoxicity or neurotoxicity after 6 months of treatment at the same DCA dose (Stacpoole et al., 2006).

Urinary concentrations of MA and δ-ALA have been used as the biochemical indicators of DCA toxicity due to their aforementioned properties. Although urinary concentrations of MA and δ-ALA were increased in children with lactic acidosis at the end of 6 months' treatment, their levels were lower than those found in tyrosinemia patients (Shroads et al., 2011). A study of S-D rats treated with DCA, 25 mg/kg/day for 5 days, reproduced a similar age-dependent toxicity and demonstrated higher concentrations of MA in both urine and plasma of old rats compared with young rats (Shroads et al., 2008). In addition to age, GSTZ1 genotype was also shown to modulate MA level in humans receiving DCA treatment. After 5 days of 25 mg/kg DCA, urinary MA was not detectable in healthy volunteers carrying at least one EGT allele but appeared in 5 out of the 6 EGT non-carriers (Shroads et al., 2011).

Hypotheses

This study has been designed to test the following hypotheses. Firstly, DCA is known to be actively taken up into the mitochondrion, where it exerts its pharmacological action by inhibiting pyruvate dehydrogenase kinase. Several members of soluble GSTs have recently been shown to dual localize in cytosol and mitochondria. We tested the hypothesis that GSTZ1 was also present in the mitochondria and the mitochondrial GSTZ1, if present, was capable of metabolizing DCA.

Secondly, age and genetic polymorphism are two major determinants of DMEs that cause altered pharmacokinetics and toxicity. The human GSTZ1 gene is known to exhibit functional polymorphisms. Given the observed differences in DCA pharmacotoxicology between children and adults, and between EGT carriers and noncarriers, we tested the hypothesis that the expression and activity of GSTZ1 were higher in children than adults, and were subject to modulation by genetic polymorphism.

Thirdly, with chloride present in liver cytosol, we failed to detect GSTZ1 inactivation under otherwise similar conditions as those reported by Tzeng et al. (2000). Chloride modulation of protein structure and activity has been documented in the literature. We thus tested the hypothesis that chloride modulated DCA-induced inactivation of GSTZ1, and that the potency of chloride modulation varied among GSTZ1 haplotypes.

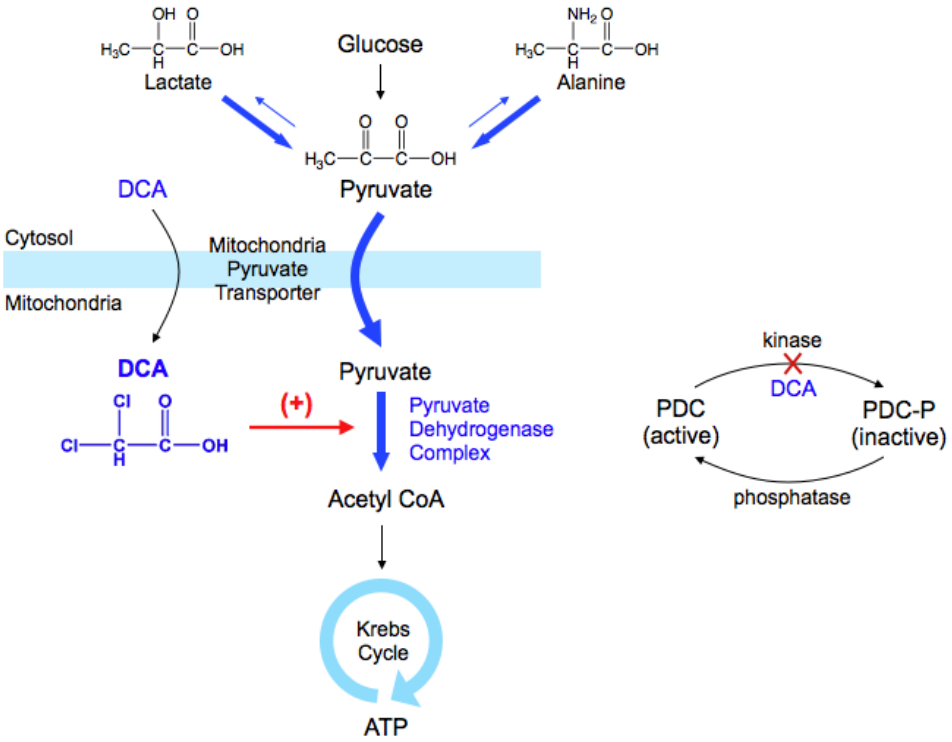

Figure 1-1. Site and mechanism of DCA action.

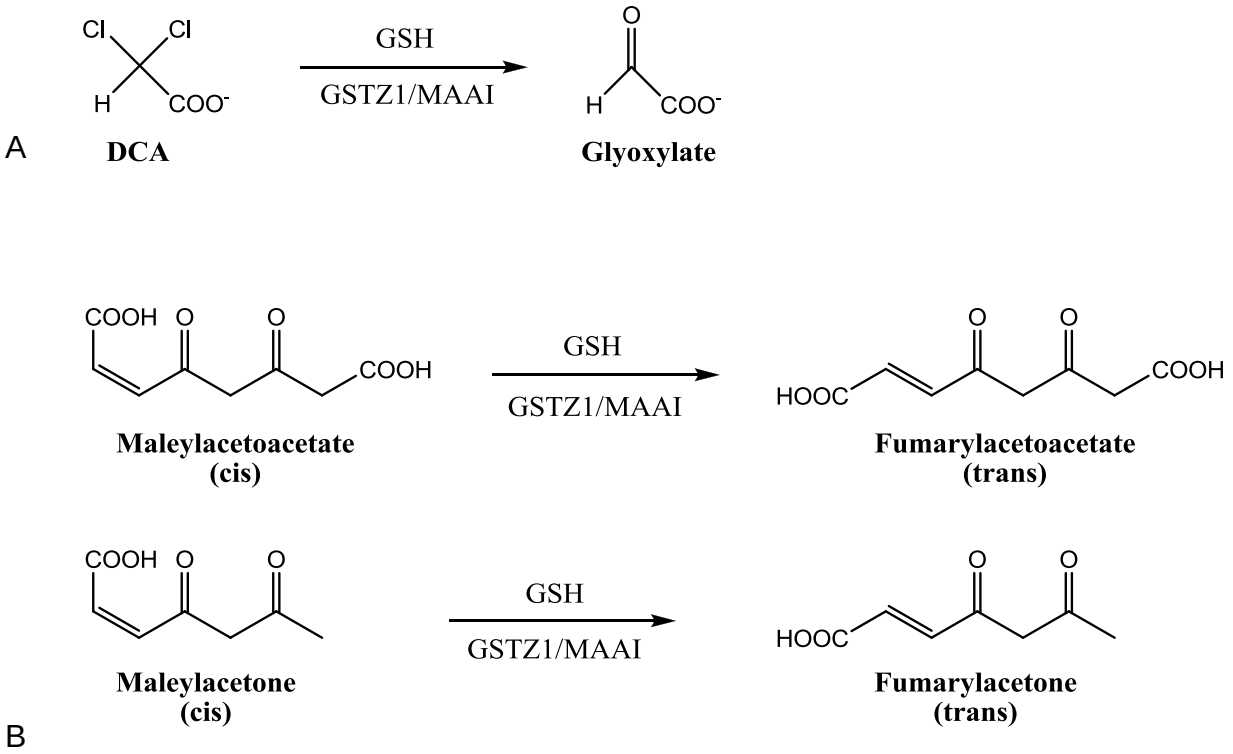

Figure 1-2. GSTZ1-catalyzed A) dechlorination of DCA to glyoxylate and B) isomerism of MAA and MA respectively to FAA and FA.

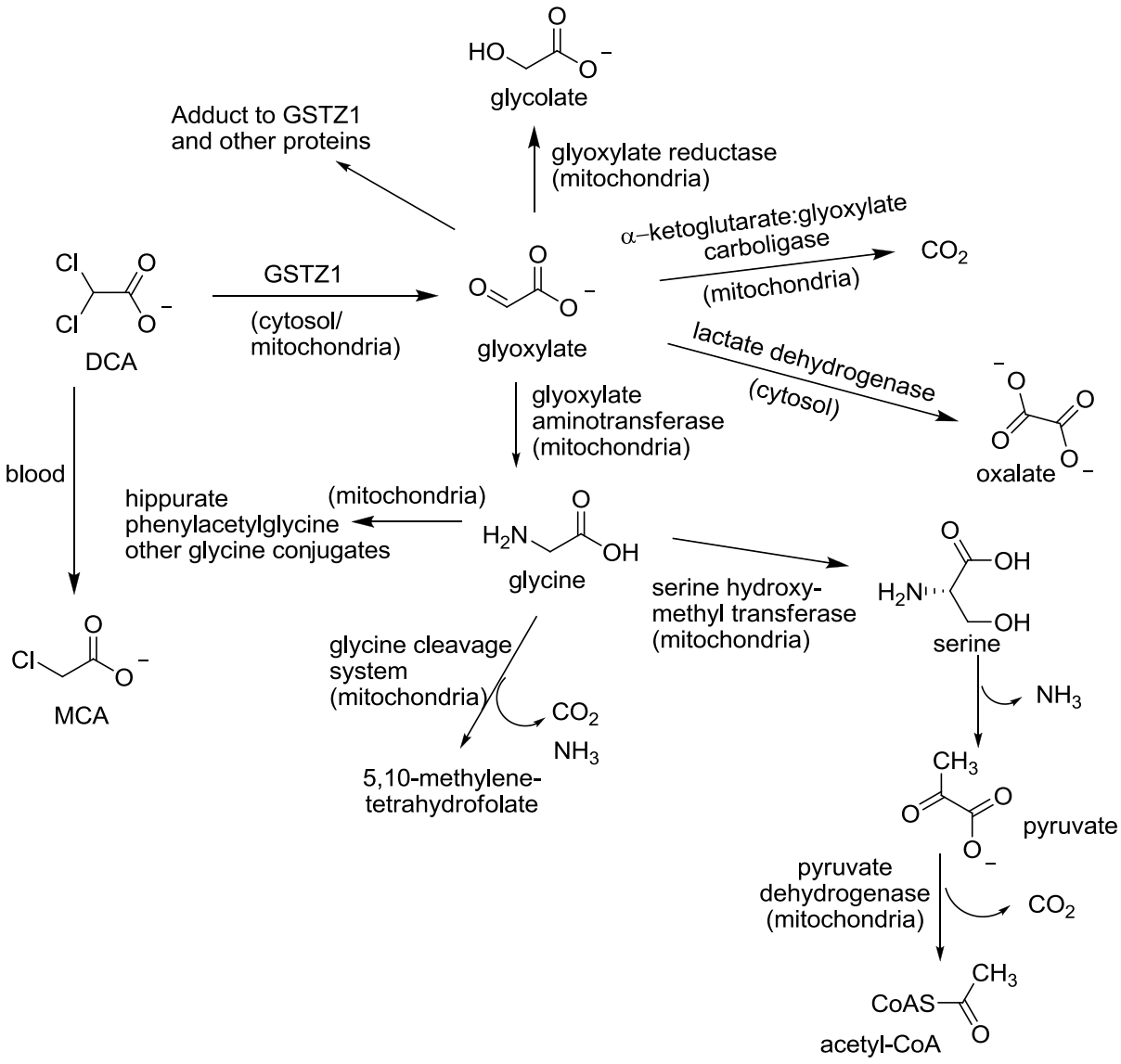

Figure 1-3. Metabolic pathways of DCA.

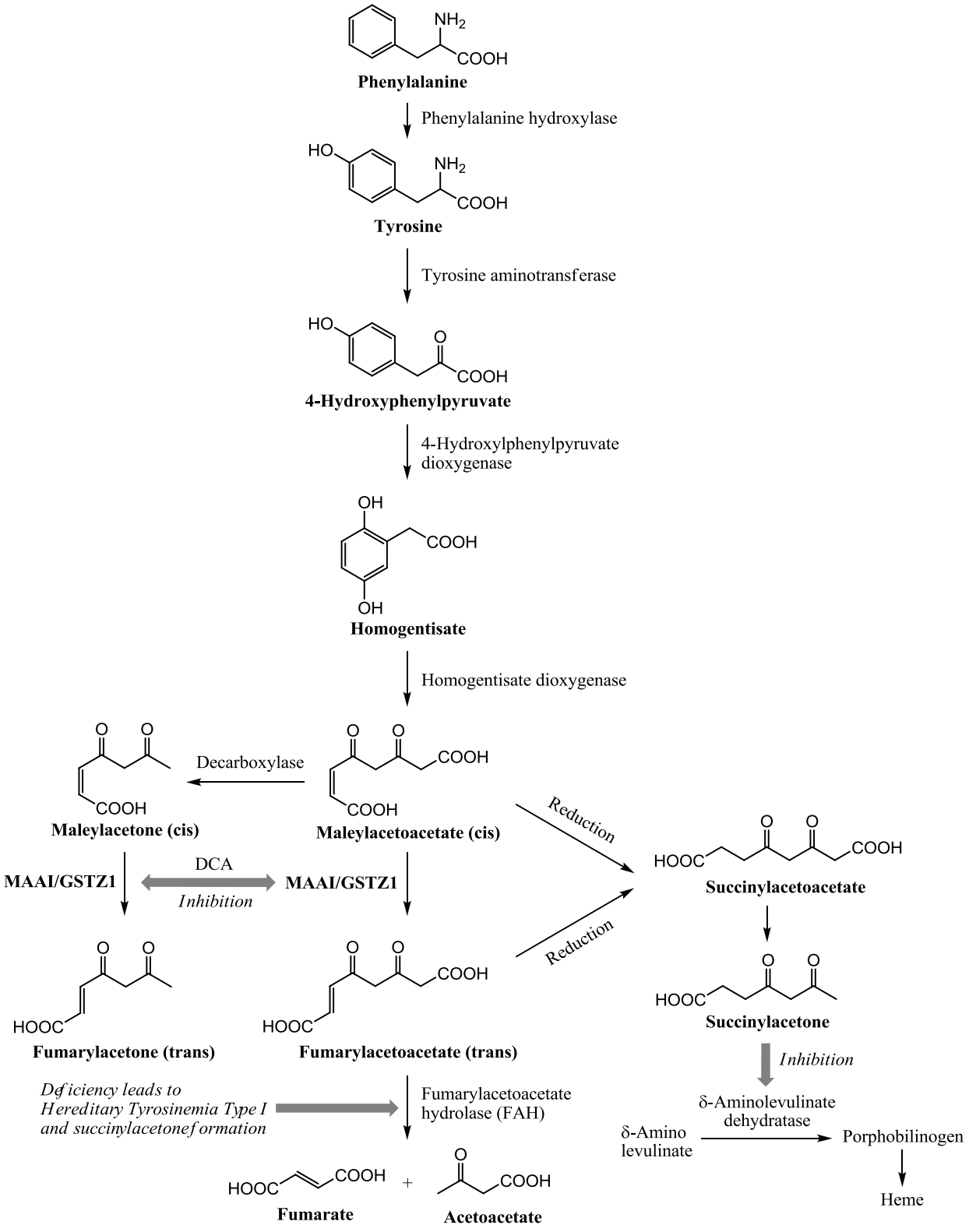

Figure 1-4. Phenylalanine/tyrosine catabolic pathways.

Table 1-1. Specific activities and inactivation half-lives of polymorphic variants of expressed recombinant hGSTZ1.

GSTZ1 Haplotype	Maleylacetone (μmol/min/mg)[a]	Chlorofluroacetate (μmol/min/mg)[a]	DCA (μmol/min/mg)[a]	Half-life of DCA inactivation (min)[b]
KRT	318 ± 91	1.35 ± 0.05	1.61 ± 0.02	23 ± 1
KGT	1010 ± 217	1.34 ± 0.03	0.45 ± 0.02	9.6 ± 0.3
EGT	1856 ± 716	1.29 ± 0.05	0.45 ± 0.03	10.1 ± 0.5
EGM	464 ± 215	1.27 ± 0.08	0.30 ± 0.025	9.5 ± 0.3

[a] Data from Blackburn et al. (2001)
[b] Data from Tzeng et al. (2000)

Table 1-2. Plasma kinetics of DCA in children and adults after single and repeated doses

Parameter	First dose		Six months	
	Children	Adults	Children	Adults
No. subjects	5	4	5	4
Age (yr)	5.2 ± 1.8	24 ± 10	5.7 ± 1.8	24.5 ± 10
Elimination $t_{1/2}$ (h)	2.5 ± 0.4	2.1 ± 1.5	6.4 ± 3.4	21 ± 5.8
C_{max} (µg/ml)	23 ± 9.1	25 ± 6.6	35 ± 10	53 ± 18
AUC (h*µg/ml)	83 ± 33	70 ± 18	340 ± 130	1500 ± 700
Clearance	150 ± 60	180 ± 46	37 ± 14	8.3 ± 4.6

Data were mean ± SD of results obtained after the first DCA dose and after 6 months of daily exposure to 12.5 mg/kg DCA every 12 h. (Adapted from Shroads et al., 2008)

Table 1-3. Pharmacokinetics of 25 mg/kg 1, 2- ^{13}C-DCA after 1 and 5 Doses in healthy adult volunteers.

			After 1st DCA Dose				After 5th DCA Dose			
Subject	Age/Sex/Race	GSTz1/MAAI Genotype	C_{max} (µg/ml)	AUC (µg/ml * min)	$t_{1/2}$ (min)	CL (ml/min)	C_{max} (µg/ml)	AUC (µg/ml * min)	$t_{1/2}$ (min)	CL (ml/min)
		EGT Carriers								
1	24/F/White	EGT/EGT	27.2	8211	79	3.04	36.1	21703	305	1.15 (2.6)*
2	25/F/White	EGT/EGT	60.3	8644	97	2.89	27.9	11705	218	2.14 (1.4)
3	24/M/White	EGT/EGT	19.4	1313	46	19.05	28.5	7899	122	3.17 (6.0)
4	23/M/Black	EGT/EGT	41.5	3689	37	6.78	32.7	12612	232	1.98 (3.4)
5	26/F/Asian	EGT/KGT	20.4	2622	36	9.54	22.6	11783	310	2.12 (4.5)
6	23/F/Black	EGT/KRT	18.1	1423	80	17.57	28.5	7934	126	3.15 (5.6)
7	25/F/White	EGT/KRT	14.4	1538	102	16.25	22.8	13715	323	1.82 (8.9)
		EGT Non-carriers								
8	25/F/White	KRT/KGT	31.8	3366	41	7.43	27.0	11746	243	2.13 (3.5)
9	37/M/White	KGT/KGT	24.7	4048	102	6.18	26.5	29214	727	0.86 (7.2)
10	33/F/White	KRT/KRT	12.4	1493	96	16.74	33.1	79525	1592	0.31 (54.0)
11	21/M/White	KRT/EGM	49.4	5301	47	4.72	35.3	98683	1774	0.25 (18.9)
12	26/M/White	KGM/KGT	27.8	78165	1264	0.32	40.8	302977	5408	0.08 (4.0)

* Values in parentheses denote fold-change in clearance (CL) between first and fifth doses.
Adapted from Shroads et al., 2011.

CHAPTER 2
MITOCHONDRION AS A NOVEL SITE OF DICHLOROACETATE BIOTRANSFORMATION BY GLUTATHIONE TRANSFERASE Z1

Specific Aim

GSTZ1 is a member of the cytosolic GST superfamily[1]. Like other GSTs, GSTZ1 is present in the cytosol and is most abundantly expressed in the liver (Lantum et al., 2002a). Over the past decade, increasing numbers of drug metabolizing enzymes have been shown to exist in multiple subcellular compartments. These include several cytosolic GSTs (GSTA1, GSTA2, GSTA4, GSTP1, and GSTM1) that were recently found to be co-localized in the hepatic mitochondria (Raza et al., 2002; Gallagher et al., 2006). Because DCA is known to be taken up by the mitochondria, we tested the postulate that this organelle is also a site of DCA biotransformation by examining the expression and activity of GSTZ1 in liver mitochondria from humans and rats.

Materials and Methods

Subcellular Fractionation of Human and Rat Livers

Adult female Sprague-Dawley (SD) rats were treated by gavage with tap water vehicle (n=9, control group) or 500 mg/kg/day DCA (n=11, DCA-treated group) for 8 weeks. Neuropathy was confirmed by measuring sciatic motor nerve conduction velocity and paw thermal response latency exactly as described elsewhere followed by sacrifice by decapitation (Calcutt et al., 2009). Studies were performed following approval by the local IACUC. De-identified normal human liver samples, 1-2 g, were collected during surgery under a protocol approved by Institutional Review Board of Shands Hospital at

[1] This work was published previously by Wenjun Li, Margaret O. James, Sarah C. McKenzie, Nigel A. Calcutt, Chen Liu, and Peter W. Stacpoole, Mitochondrion as a Novel Site of Dichloroacetate Biotransformation by Glutathione Transferase ζ1, *J Pharmacol Exp Ther* 2011 336:87-94.

the University of Florida (Gainesville, FL) for use in these studies. Livers were quickly removed, snap-frozen in liquid nitrogen and stored at -80°C until use.

Frozen liver was thawed and rinsed in ice-cold homogenizing buffer (0.25 M sucrose, 0.02 M Hepes-NaOH pH 7.4 and 0.1 mM phenylmethanesulfonyl fluoride). Rinsed livers were minced and homogenized in 5 volumes of homogenizing buffer with a motor-driven Teflon pestle for 4 complete strokes. After sedimenting the nuclei and cell debris at 600 X g, mitochondria were pelleted by centrifuging the supernatant at 13,000 X g for 20 min. The 13,000 x g supernatant was further subjected to differential centrifugation to isolate cytosol and washed microsomes (James et al., 1976). The mitochondrial pellet was resuspended and washed twice before being taken up in the resuspension buffer (0.25 M sucrose, 0.01 M Hepes-NaOH pH 7.4, 0.1 mM dithiothreitol, 0.1 mM EDTA, 0.1 mM phenylmethanesulfonyl fluoride and 5% glycerol) in a volume equal to the liver weight. The washed mitochondria and cytosol were stored in aliquots at -80°C until use. All procedures were performed at 4°C or on ice. Cytosol and mitochondria were dialyzed with 10 kD MWCO Slide-A-Lyzer® Dialysis Cassettes (Thermo Scientific, Rockford, IL) against 1.15% KCl and 0.05 M potassium phosphate buffer pH 7.4 before use for assays. Protein concentrations were determined by the Bradford method (Bio-Rad, Hercules, CA) using bovine serum albumin (BSA; Sigma-Aldrich, St. Louis, MO) as protein standard.

Subfractionation of Liver Mitochondria

Three 9-week old male SD rats were killed by decapitation and their livers were quickly isolated and rinsed in ice-cold homogenizing buffer to remove blood. The washed mitochondria were immediately isolated by procedures described above and subfractionated as follows. The suspension of washed mitochondria was diluted with

swelling buffer (0.01 M Tris-HCl pH 7.4) to a final sucrose concentration of ~0.05 M and gently mixed with a magnetic stirrer at 4°C for 15 min. Shrinking buffer (2 M sucrose, 100 mM Tris-HCl pH 7.4) was then added to the swelled mitochondria to give a final sucrose concentration of ~0.3 M. After another 15 min stirring, the swollen-and-shrunk (shocked) mitochondria were centrifuged at 20,000 X g for 20 min. The supernatant yielded the intermembrane space (IMS) proteins. The pellet of shocked mitochondria was washed once, resuspended in homogenizing buffer and stored at -80°C. After 3 cycles of freezing-and-thawing, the shocked mitochondria were further subjected to 3 strokes of homogenization by a Dounce homogenizer and 5 cycles of 5 sec sonication at 25 sec intervals. The shocked mitochondria were then centrifuged at 125,000 X g for 60 min to sediment the total mitochondrial membrane with the mitochondrial matrix remaining in the supernatant. The pellet containing the total mitochondrial membrane was resuspended in resuspension buffer. The IMS protein and matrix protein were concentrated by filtering through Amicon Ultra – 15 ml filters of 10 kD MWCO (Millipore, Billerica, MA).

Electrophoresis and Western Blots

Known amounts of denatured protein were separated on 4-15% SDS-PAGEs (Tris-HCl Gel, Bio-Rad) and subsequently electrotransferred onto polyvinylidene fluoride membrane (PVDF, Millipore). Purified recombinant human GSTZ1C-1C was obtained as previously described (Guo et al., 2006) and used as positive control. After blocking, the membrane was incubated overnight at 4°C with primary antibodies, 1:2000 rabbit polyclonal anti-hGSTZ1C-1C (Cocalico Biologicals, Inc., Reamstown, PA), 10.2 μg/ml mouse monoclonal MitoProfile® Membrane Integrity WB Antibody Cocktail (MitoSciences, Eugene, OR) or 1:2000 rabbit monoclonal anti-ALDH1A1 (Abcam,

Cambridge, MA). The membrane was then washed and incubated with the corresponding secondary antibodies, horseradish peroxidase conjugated donkey anti-rabbit IgG, 1:2000 or sheep anti-mouse IgG $F(ab')_2$ 1:5000 (GE healthcare, Piscataway, NJ). Protein signal was developed by Pierce® ECL substrate (Thermo Scientific) on Amersham Hyperfilm™ ECL (GE healthcare) according to manufacturers' instructions. For quantitative analysis, the resulting hyperfilm was digitized by scanning and the density of bands was quantitated by ImageJ software (version 1.41o, National Institute of Health, USA).

GSTZ1 Activity

The specific activity of GSTZ1 was measured using [1-^{14}C]-DCA (American Radiolabeled Chemicals, Inc., St. Louis, MO) as substrate and assay products were measured by an HPLC method coupled with radiochemical detection (James et al., 1997). Assay conditions were optimized to achieve linearity of product formation with incubation time and protein concentration; substrate consumption did not exceed 15%. To determine the maximum reaction rate, assay tubes containing 0.2 mM ^{14}C-DCA in 0.1 M Hepes-NaOH pH 7.6 were incubated with either cytosolic protein and 2 mM GSH or mitochondrial protein and 5 mM GSH in a volume of 0.1 ml. After a 2-min pre-incubation at 37°C, the reaction was started by adding ^{14}C-DCA. Tubes were incubated at 37^{o}C with gentle shaking for 15 min, after which the reaction was stopped by adding 0.1 ml ice-cold methanol. For the sub-mitochondrial experiment, enzyme specific activity was measured with 0.2 mM DCA and 2 mM GSH over 30-min incubation for all fractions. For kinetic studies cytosol and mitochondria were incubated with varying concentrations of GSH and DCA over adjusted incubation times, as specified in the results. The kinetic parameters (V_{max} and K_m) were derived with the software GraphPad

Prism version 4.03 (San Diego, CA) by fitting the data to the Michaelis-Menten equation, $V = V_{max}[S]/(K_m + [S])$. Goodness of fit to the Michaelis-Mention equation was determined by the software.

Immunoprecipitation of Mitochondrial GSTZ1

Soluble mitochondrial protein of human liver and mitochondrial matrix protein of rat liver were used for immunoprecipitation of GSTZ1. To obtain the soluble mitochondrial protein of human liver, the washed human liver mitochondria were frozen and thawed three times, and then diluted to about 2 mg/ml in homogenizing buffer. After sonication and homogenization, the disrupted mitochondria were centrifuged at 125,000 X g for 60 min to pellet the total mitochondrial membrane. The soluble mitochondrial protein was collected from the supernatant and further concentrated using Amicon Ultra – 15 ml filters of 10 kD MWCO.

Immunoprecipitation of mitochondrial GSTZ1 was carried out using the Pierce® Direct IP kit (Thermo Scientific) following the provider's instructions. For each column, 10 µg of hGSTZ1C-1C antibody was coupled to 30 µl of a 50% slurry of AminoLink® Plus coupling resin. Mitochondrial protein, 500 µg, was incubated with the antibody-coupled resin overnight at 4°C. After centrifuging the mixture to remove unbound proteins, the resin was washed with IP lysis/wash buffer supplied by the kit. The antigen was then eluted with the primary amine-containing, pH 2.8 elution buffer supplied by the kit. Eluants were neutralized with 1 M Tris-HCl pH 9.5 in a 10:1 ratio. For each species, eluants from three columns were pooled and concentrated through Amicon Ultra - 0.5 ml filters of 10 kD MWCO (Millipore). The concentrated eluants were denatured and separated on 4-15% SDS-PAGEs. Protein bands from the rat or human samples that

migrated to the same position as the positive control, purified hGSTZ1C, were excised and digested with trypsin (Sheffield et al., 2006) for LC-MS/MS protein identification.

LC-MS/MS

The trypsin digested samples were injected onto a capillary trap (LC Packings® PepMap; Dionex Corporation, Sunnyvale, CA) and washed for 5 min with a flow rate 10 µl/min of 0.1% v/v acetic acid. The samples were loaded onto a LC Packings® C18 PepMap HPLC column (Dionex Corporation, Sunnyvale, CA). The elution gradient of the HPLC column started at 97% solvent A (0.1% v/v acetic acid, 3% v/v acetonitrile and 96.9% v/v water), 3% solvent B (0.1% v/v acetic acid, 96.9% v/v acetonitrile and 3% v/v water) and finished at 40% solvent A, 60% solvent B for 60 min. LC-MS/MS analysis was carried out on a hybrid quadrupole-TOF mass spectrometer (QSTAR, Applied Biosystems, Framingham, MA). The focusing potential and ion spray voltage were set to 275 V and 2600 V, respectively. The information-dependent acquisition (IDA) mode of operation was employed in which a survey scan from m/z 400–1200 was acquired followed by collision induced dissociation of the three most intense ions. Survey and MS/MS spectra for each IDA cycle were accumulated for 1 and 3 sec, respectively.

Protein Search Algorithm

Tandem mass spectra were extracted by ABI Analyst version 1.1. All MS/MS samples were analyzed using Mascot (Matrix Science, London, UK; version 2.2.2). Mascot was set up to search the International Protein Index (IPI) database with trypsin as the digestive enzyme. Mascot was searched with a fragment ion mass tolerance of 0.30 Da and a parent ion tolerance of 0.30 Da. Iodoacetamide derivatization of Cys, deamidation of Asn and Gln, oxidation of Met were specified in Mascot as variable modifications. Scaffold 2 (version Scaffold-02.03.01, Proteome Software Inc., Portland,

OR) was used to validate MS/MS based peptide and protein identifications. Peptide identifications were accepted if they could be established at greater than 95.0% probability, as specified by the Peptide Prophet algorithm (Keller et al., 2002). Protein identifications were accepted if they could be established at greater than 99.0% probability and contained at least 2 identified unique peptides. Protein probabilities were assigned by the Protein Prophet algorithm (Nesvizhskii et al., 2003).

Results

Expression and Activity of GSTZ1 in Hepatic Mitochondria

In liver mitochondria of both human and rat, our hGSTZ1 antibody cross-reacted with a protein that migrated similarly to the purified hGSTZ1 and the cytosolic GSTZ1 at ~24 kD (Figure 2-1). GSTZ1 immunoreactivity was more intense in cytosol than in mitochondria for a given amount of protein, indicating a more abundant expression of GSTZ1 in cytosol. To assure that the detection of mitochondrial immunoreactive GSTZ1 was not due to cytosolic contamination, mitochondrial purity was established by demonstrating minimal detection of the cytosolic marker aldehyde dehydrogenase 1A1 (ALDH1A1). Cytosolic expression of GSTZ1 was 2.4-fold and 3.9-fold higher than mitochondrial in human and rat livers, respectively, on a per milligram of protein basis (Table 2-1). This is consistent with the 2.5 – 3-fold higher activity of GSTZ1 in cytosol than in mitochondria, as determined using ^{14}C-DCA as substrate. About 86% [human: 40.1/(40.1+6.78); rat: 0.92/(0.92+0.14)] of cellular GSTZ1 was located in cytosol and 14% was located in mitochondria, based on the higher yield of protein from cytosol than mitochondria and assuming that 30 mg mitochondria were present per gram liver (Fleischer et al., 1979).

GSTZ1 is known to be inactivated by DCA after repeated exposure (Cornett et al., 1999). This was confirmed by the marked reduction in both the expression and activity of cytosolic GSTZ1 in rats treated with DCA 500 mg/kg/day for 8 weeks (Figure 2-1 and Table 2-1). The expression of mitochondrial GSTZ1 in these rats was also reduced to ~10% of control levels and the specific activity was reduced to below the detection limit (Table 2-1). Coincidentally, we observed a strong induction of cytosolic marker ALDH1A1 in the DCA-treated rats compared to control rats.

Our GSTZ1 antibody cross-reacted with an unknown protein in rat mitochondria that appeared 1 – 2 kD larger than GSTZ1 on SDS-PAGE (Figure 2-1). The cytosolic expression of this cross-reacting protein changed from not detectable in fresh control livers to barely detectable in frozen control livers to readily-detectable in frozen DCA-treated livers (Figure 2-2). This pattern of expression is similar to those of mitochondrial matrix protein cyclophilin D (CypD) and intermembrane space protein cytochrome C (CytC). Preliminary investigation of this protein by immunoprecipitation and LC-MS/MS protein identification suggested that it was a mitochondrial matrix protein with less than 3% sequence identity to hGSTZ1 (NCBI Blastp). This result was further supported by its submitochondrial localization in the matrix (see below, Figure 2-4A)

Mitochondrial GSTZ1 Is Localized in the Matrix

The mitochondrion has a double membrane structure that divides the organelle into four compartments: the outer membrane (OM), the intermembrane space (IMS), the inner membrane (IM) and the matrix (Figure 2-3). To investigate if DCA biotransformation occurs in the same mitochondrial compartment as its pharmacodynamic action, we examined GSTZ1 expression and activity in the washed mitochondria and three sub-mitochondrial fractions: IMS, the matrix and the membranes

(including OM and IM) (Figure 2-4). GSTZ1 expression and catalytic activity were greatest in the matrix, being nearly 3 times higher than in washed mitochondria. Low levels of GSTZ1 expression and activity were found in the membrane fraction, which might be due to incomplete release of matrix protein from the shocked mitochondria during fractionation. However, neither expression nor activity was detectable in the IMS. We also confirmed that GSTZ1 exists in cytosol, but not microsomes. Similar levels of GSTZ1 expression were detected in cytosol and mitochondrial matrix. However, the cytosolic marker ALDH1A1 was only detected in cytosol but not in mitochondrial matrix. This also indicated that the presence of GSTZ1 in mitochondria was not due to cytosolic contamination.

LC-MS/MS Identification of the Mitochondrial GSTZ1

The identity of the mitochondrial GSTZ1 was verified by immunoprecipitating the antibody-reactive proteins from human and rat liver mitochondria and analyzing the tryptic peptide sequences by LC-ESI-QTOF. We used the matrix protein of rat mitochondria and the soluble protein of human mitochondria for immunoprecipitation. The immunoprecipitated GSTZ1 of human liver mitochondria was identified with 3 unique peptides in 4 unique spectra, covering 12% (27/216) of the hGSTZ1 protein sequence (Figure 2-5 and Table 2-2). Although the coverage was relatively low, a clear ladder of fragmentation was shown in the peptide, ^{41}DGGQQFSK^{48} (Figure 2-6), which increased our confidence of the protein identification. Of the immunoprecipitated rat GSTZ1, 2 unique peptides covering 13% (28/216) of the rat GSTZ1 protein sequence were identified (Figure 2-5 and Table 2-2).

Kinetic Study of Cytosolic and Mitochondrial GSTZ1

Rat mitochondrial GSTZ1 had a 2.5-fold higher $^{App}K_m$ for GSH than the cytosolic GSTZ1, whereas the $^{App}K_m$s for DCA were identical (Table 2-3). With either GSH or DCA as the variable substrate, the $^{App}V_{max}$ values of cytosolic GSTZ1 were 3 times those of mitochondrial GSTZ1, in good accordance with the 3.9-fold higher expression of cytosolic GSTZ1 per mg protein (Table 2-1). Lineweaver-Burk plots of cytosolic GSTZ1 and mitochondrial GSTZ1 with GSH and DCA as substrates were shown for one representative rat in Figure 2-7.

Discussion

The mitochondrion is the primary site of DCA's pharmacodynamic action. However, its role in DCA biotransformation has been largely overshadowed by the prominence of cytosol and endoplasmic reticulum in drug metabolism. In this study we demonstrate the mitochondrion to be a second site of DCA biotransformation in a reaction catalyzed by GSTZ1, an enzyme co-localized in the mitochondrial matrix and cytosol. Furthermore, GSTZ1 expression and activity in the liver mitochondria are susceptible to DCA inactivation, as occurs with the cytosolic form of GSTZ1. We also verified partial sequences of mitochondrial GSTZ1 by LC-MS/MS and compared the kinetics between cytosolic and mitochondrial GSTZ1 using DCA and GSH as substrates.

The level of GSTZ1 expression is similar in cytosol and mitochondrial matrix, whereas it is about 70% less in intact mitochondria on a per milligram-of-protein basis. Although a low level of cytosolic contamination was to be expected in the liver mitochondria isolated by differential centrifugation, we confirmed the authenticity of mitochondrial GSTZ1 by demonstrating minimal co-detection of cytosolic marker

ALDH1A1. Moreover, we would expect to detect any cytosol-originated GSTZ1 in the IMS fraction, which was obtained from the first supernatant of osmotically-shocked mitochondria. In fact, GSTZ1 was detected in the mitochondrial matrix at an intensity similar to that in cytosol, but without detectable ALDH1A1 (Figure 2-4). This evidence firmly established the mitochondrial origin of GSTZ1. In light of this finding, we searched the literature for GSTZ1 identification from studies of mitochondrial proteome. Indeed, GSTZ1 was identified in the mitochondrial proteome of mouse liver, heart, and kidney (Mootha et al., 2003). Consistent with our finding, GSTZ1 was shown in the proteome of mitochondrial matrix but not inter-membrane space of rat liver (Forner et al., 2006).

Proteins targeted to the mitochondrial matrix usually possess a 15-40 amino-acid long presequence at the N-terminal that forms an amphipathic helix to interact with mitochondrial transport machinery during translocation and the presequence is often cleaved off upon import. A few matrix targeting proteins with non-cleaved presequences or C-terminal presequences have also been identified (Pfanner and Geissler, 2001). All GSTs (GSTA1, GSTA2, GSTA4, GSTP1 and GSTM1) that are currently known to co-localize in cytosol and mitochondrial matrix have similar molecular sizes and identical N-terminals in both compartments (Raza et al., 2002; Gallagher et al., 2006). Mitochondrial import studies of GSTA4 and GSTM1 suggest non-cleaved internal targeting sequences at the C-terminal and N-terminal, respectively, of the mature GST proteins (Robin et al., 2003; Goto et al., 2009). Furthermore, protein kinase A (PKA)- and protein kinase C (PKC)-catalyzed phosphorylation has been shown to facilitate GSTA4 translocation to the matrix (Robin et al., 2003). The present study of cytosolic and mitochondrial GSTZ1 also suggests their similar molecular weights, as shown by

the indistinguishable rates of migration on SDS-PAGEs. To obtain more insight into protein structure, we attempted direct N-terminal sequencing for human mitochondrial GSTZ1 immobilized on PVDF membrane. However, the study failed due to the blocked N-terminus, which was also observed for rat cytosolic GSTZ1 (Tong et al., 1998b). On the other hand, one tryptic peptide of human mitochondrial GSTZ1 identified by LC-MS/MS shared the same identity as the C-terminal amino acids of cytosolic GSTZ1, suggesting that the C-terminus of GSTZ1 remained intact after mitochondrial import. Therefore, if a mitochondrial targeting sequence of GSTZ1 exists, it may reside within the mature protein and not undergo proteolysis upon import.

GSTZ1 of both cytosol and mitochondria catalyzes GSH-dependent dechlorination of DCA, exhibiting the same $^{App}K_m$s (0.033 mM) for DCA, but a 2.5-fold difference in $^{App}K_m$s for GSH (0.50 mM mitochondria vs 0.19 mM cytosol). Of cytosolic GSTZ1, the $^{App}K_m$ for GSH obtained currently using female SD rats is 2.5-fold higher than we previously reported using male SD rats (James et al., 1997) and is 3.2-fold higher than Tong's study using male Fisher 344 rats, in which a 2-fold higher $^{App}K_m$ for DCA was also found (Tong et al., 1998a). The higher $^{App}K_m$ for GSH observed with mitochondrial GSTZ1 suggests that it has a weakened access or binding to GSH compared to its cytosolic counterpart. Inspection of the crystal structure of hGSTZ1A-1A with GSH revealed that GSH was bound in a deep crevice with close interaction with the active site residues Ser14-Ser15-Cys16 near the N-terminus (Polekhina et al., 2001). Cys16 was found to be particularly important in maintaining proper binding and orientation with GSH. Mutation of Cys16 to Ala caused dramatic increases in K_ms for GSH with various substrates (Board et al., 2003; Ricci et al., 2004). As demonstrated in mouse GSTA4,

the mitochondrial form is more heavily phosphorylated than the cytosolic form while possessing the same primary protein sequence (Robin et al., 2003). If post-translational modification is involved in the GSTZ1 translocation to mitochondria, modifications of residues around the GSH binding pocket may alter the conformation of this region in mitochondrial GSTZ1 and thus contribute to the reduced GSH affinity. Nevertheless, GSH is present at concentrations (2-10 mM) well above the K_m values in cytosol and mitochondria (Hansen et al., 2006); therefore, the difference in K_m for GSH should not affect or limit the rates of DCA dechlorination in either compartment under physiological conditions.

Inspection of the DCA metabolic pathway reveals that all but one of the enzymes involved in secondary biotransformation are located in the mitochondria (Figure 1-3). Our study establishes a novel role of the mitochondrion in DCA primary biotransformation, which may allow efficient degradation of glyoxylate in mitochondria and therefore explain the fact that a large majority of DCA metabolites observed *in vivo* are derived from mitochondrial pathways of secondary biotransformation (Lin et al., 1993; James et al., 1998). However, generation of glyoxylate in the mitochondria may perturb the mitochondrial redox homeostasis because glyoxylate is an electrophile and may react with cellular macromolecules (Anderson et al., 2004). DCA-induced inactivation of GSTZ1 was observed in both cytosol and mitochondria of rats treated with 500 mg/kg/day of DCA for 8 weeks. However, the question remains as to whether or not lower environmental and therapeutic doses of DCA would affect GSTZ1 similarly in the two compartments.

We unexpectedly observed a marked induction of cytosolic ALDH1A1 in the livers of DCA-treated rats, which we speculate to be caused by an increased level of oxidative stress in the livers due to DCA treatment. ALDH1A1 is a cytosolic and inducible isoform of the aldehyde dehydrogenase family that catalyzes the oxidation of medium-chain aliphatic aldehydes, including 4-hydroxynonenal and malondialdehyde (Alnouti and Klaassen, 2008). This is noteworthy because elevated levels of these indices of lipid peroxidation have recently been found in the sciatic nerves of rats treated with the same dose of DCA as used in the present study (Calcutt et al., 2009). Furthermore, increased production of reactive oxygen species and lipid peroxidation have been demonstrated in the livers of mice treated with high doses of DCA (Larson and Bull, 1992; Hassoun et al., 2010). Overexpression of ALDH1A1 has been shown to be an adaptive response to oxidative stress (Choudhary et al., 2005; Leonard et al., 2006). Therefore, we tentatively attribute the induced expression of cytosolic ALDH1A1 to be a secondary response to DCA exposure.

The GSTZ1 antibody-cross-reacting protein was shown to be a rat mitochondrial matrix protein but exhibited varying degrees of expression in the cytosol depending on the liver condition. Its appearance in the cytosol of frozen control liver could be due to mitochondrial membrane lesions caused by freezing the liver and thawing it on ice (Pallotti and Lenaz, 2007). It is notable that the expression of this protein was further increased in the DCA-treated cytosol. We speculate that this altered expression is a combined result of freeze-thawing the liver and further leakage of mitochondrial protein due to DCA treatment. DCA can induce oxidative stress (Larson and Bull, 1992;

Hassoun et al., 2010), a condition detrimental to mitochondrial membrane integrity (Fulda et al., 2010).

In conclusion, we demonstrate that the mitochondrion, known to be the site of DCA's pharmacological action on PDC, is also a site of DCA biotransformation. The reaction is catalyzed by GSTZ1, an enzyme co-localized in the cytosol and the mitochondrial matrix. GSTZ1 of both compartments is inactivated by high doses of DCA and exhibits the same $^{App}K_m$s for DCA, but different $^{App}K_m$s for GSH. The discovery of this organelle as a second site of DCA biotransformation provides a new perspective on understanding DCA metabolism.

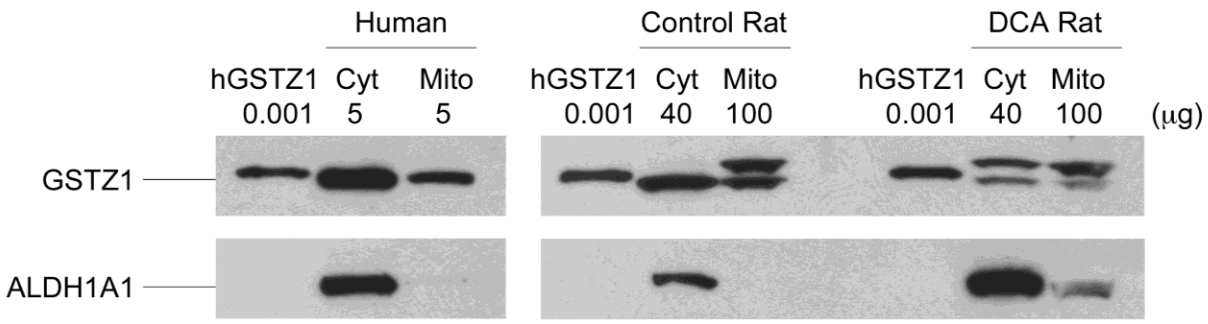

Figure 2-1. Representative Western blot of immunoreactive GSTZ1 in the liver cytosol and mitochondria of human, control rat, and DCA rat. Shown are cytosol and mitochondria of one individual from each group. The DCA rat was exposed to 500 mg/kg/day DCA for 8 weeks before preparation of subcellular fractions. A rabbit polyclonal antibody against human GSTZ1C-1C was used. Aldehyde dehydrogenase 1A1 (ALDH1A1) was used as a cytosolic marker to monitor mitochondria purity. hGSTZ1, purified recombinant human GSTZ1C-1C. Protein loading of each sample is indicated on the figure.

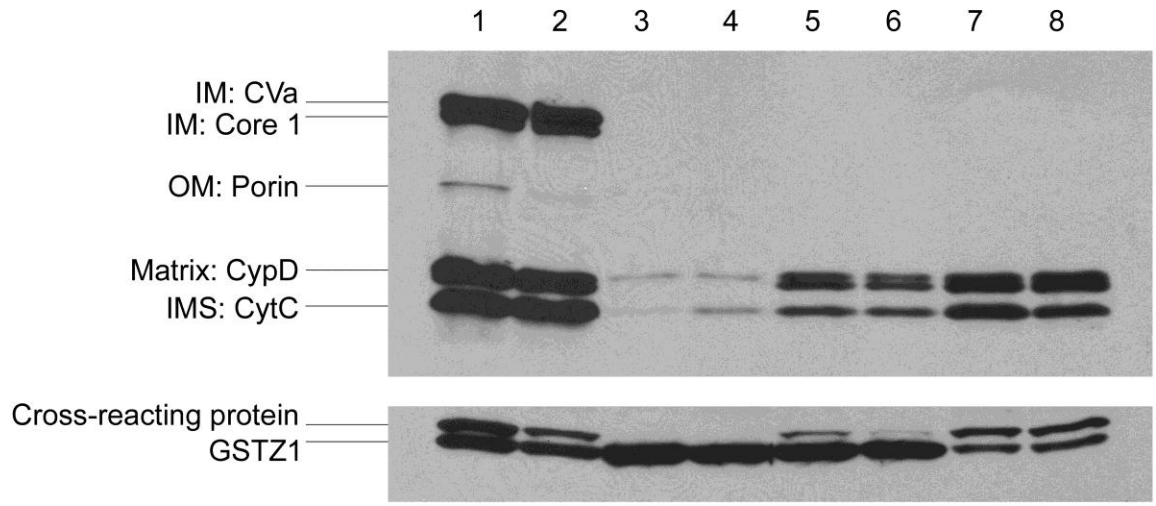

Figure 2-2. The expression of GSTZ1 and the cross-reacting protein in the mitochondria (lanes 1 and 2) and cytosol (lanes 3 and 4) isolated from fresh livers of control rats, and in the cytosol isolated from frozen livers of control (lanes 5 and 6) and DCA-treated (lanes 7 and 8) rats (500 mg DCA/kg/day for 8 weeks). The lower film was exposed for a prolonged period of time to show the change in the expression of the cross-reacting protein. Complex V subunit a (CVa) and Complex III subunit Core 1 are protein markers for mitochondrial inner membrane (IM), Porin for mitochondrial outer membrane (OM), Cyclophilin D (CypD) for mitochondrial matrix, and Cytochrome C (CytC) for mitochondrial intermembrane space (IMS). Results from two rats are shown for each group. Each lane contains equal amounts of protein.

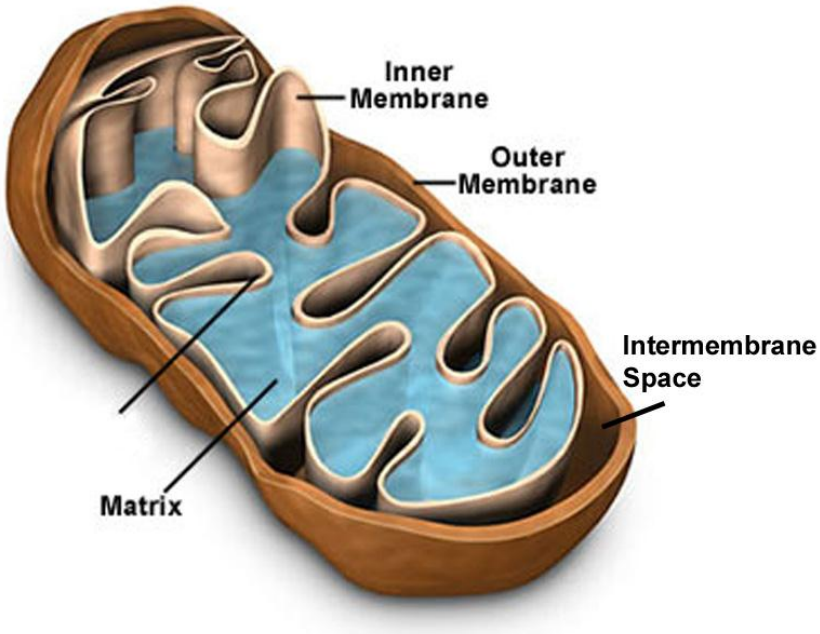

Figure 2-3. Structure of the mitochondrion. (Copyright © by Molecular Expressions™. Reproduced with permission.)

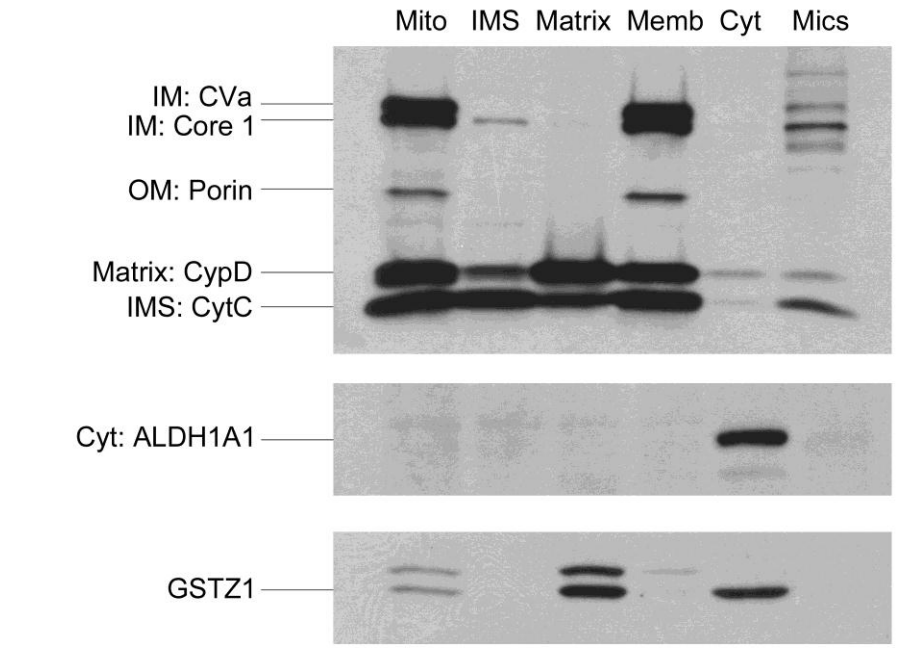

A

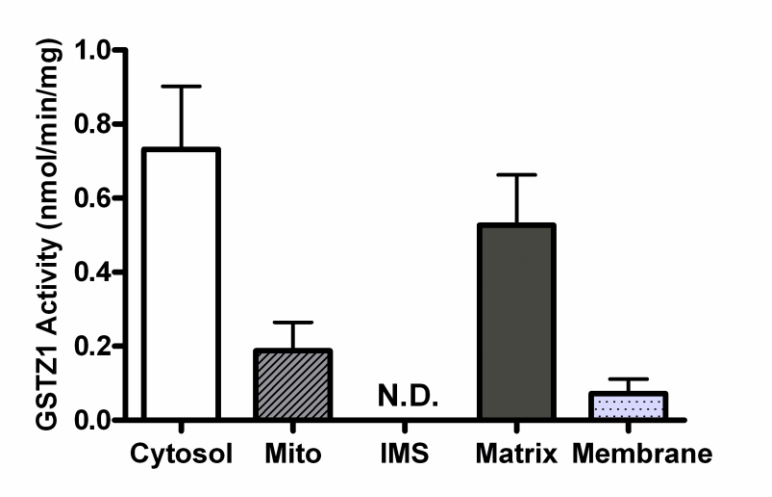

B

Figure 2-4. Enrichment of GSTZ1 expression and activity in the matrix of rat liver mitochondria. A) Representative Western blot of GSTZ1 expression in the subcellular and sub-mitochondrial fractions of rat liver. Each fraction was loaded with equal amounts of protein and the fraction identities were confirmed by the predominant expression of respective marker proteins: ALDH1A1 for cytosol (Cyt), Complex V subunit a (CVa) and Complex III subunit Core 1 for mitochondrial inner membrane (IM), Porin for mitochondrial outer membrane (OM), Cyclophilin D (CypD) for mitochondrial matrix, and Cytochrome C (CytC) for mitochondrial intermembrane space (IMS). Mito., washed mitochondria; Memb., mitochondrial membranes; Mics., microsomes. B) GSTZ1 activity in the cytosol and sub-mitochondrial fractions of rat livers measured with 0.2 mM 14C-DCA as substrate. Data are shown as mean ± S.D. of 3 rats. N.D., not detectable.

A

MQAGKPILYS YFRSSCSWRV RIALALKGID YETVPINLIK **DGGQQFSKDF**
QALNPMKQVP TLKIDGITIH QSLAIIEYLE EMRPTPRLLP QDPKKRASVR
MISDLIAGGI QPLQNLSVLK QVGEEMQLTW AQNAITCGFN ALEQILQSTA
GIYCVGDEVT MADLCLVPQV ANAERFKVDL TPYPTISSIN KRLLVLEAFQ
VSHPCR**QPDT** **PTELRA**

B

MQAGKPVLYS YFRSSCSWRV RIALALKGID YEIVPINLIK **DGGQQFSEEF**
QTLNPMKQVP ALKIDGITIG QSLAILEYLE ETRPIPRLLP QDPQKRAIVR
MISDLIASGI QPLQNLSVLK QVGQENQMPW AQK**AITSGFN** **ALEK**ILQSTA
GKYCVGDEVS MADVCLAPQV ANAERFKVDL SPYPTISHIN KALLALEAFQ
VSHPCRQPDT PAELRT

Figure 2-5. LC-ESI-QTOF analysis of the tryptic peptides of human and rat mitochondrial GSTZ1. A) Amino acid sequence of human GSTZ1 (NCBI accession no. NP_665877). B) Amino acid sequence of rat GSTZ1 (NCBI accession no. NP_001102915). Peptide fragments identified by MS are highlighted in yellow and modified amino acids are highlighted in green.

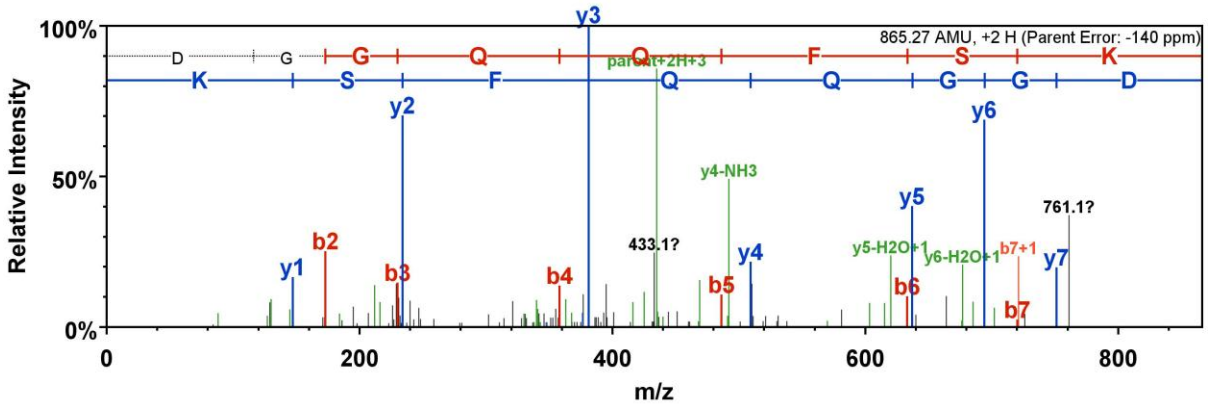

Figure 2-6. MS/MS fragmentation of the peptide ^{41}DGGQQFSK^{48} of human mitochondrial GSTZ1.

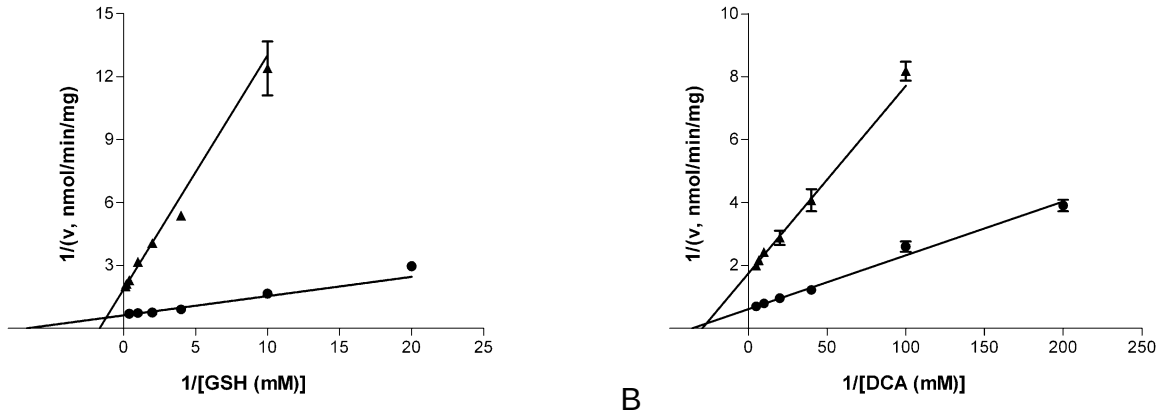

Figure 2-7. Lineweaver-Burk plots of the rate of DCA biotransformation (v) versus the concentrations of A) cosubstrate GSH and B) substrate DCA in the liver cytosol (●) and mitochondria (▲).The lines were constructed using K_m and V_{max} values obtained from Michaelis-Menten equation, and intercept $1/V_{max}$ on Y axis and $-1/K_m$ on X axis. Data are shown as mean ± SEM of assay duplicates from one representative rat.

Table 2-1. Expression and activity of GSTZ1 in the liver cytosol and mitochondria of human, control rat, and DCA rat.

	GSTZ1 expression per gram liver[a]		GSTZ1 expression per mg protein[a]		GSTZ1 activity (nmol/min/mg)[c]	
	Cytosol[b]	Mitochondria[b]	Cytosol	Mitochondria	Cytosol	Mitochondria
Human (n=4)	40.1 ± 11.8	6.78 ± 1.11	0.54 ± 0.10	0.23 ± 0.04	0.49 ± 0.08	0.20 ± 0.07
Control rat (n=4)	0.92 ± 0.06	0.14 ± 0.01	0.94 ± 0.07	0.24 ± 0.02	1.47 ± 0.09	0.48 ± 0.02
DCA rat (n=4)	0.11 ± 0.03	0.012 ± 0.003	0.10 ± 0.02	0.021 ± 0.006	0.11 ± 0.06[d]	N.D.

[a] GSTZ1 expression was analyzed using 5 μg human cytosol, 5 μg mitochondria, 40 μg rat cytosol and 100 μg rat mitochondria on Western blots probed with hGSTZ1 polyclonal antibody. Band intensity was quantitated by ImageJ software. For human samples, the amounts of GSTZ1 were quantitated by comparing the immuno-intensity to a standard curve constructed with pure hGSTZ1. Data are shown as μg hGSTZ1 / g liver or μg hGSTZ1 / mg protein. For rat samples, individual GSTZ1 expression was normalized as a fraction of one control cytosol that had highest level of GSTZ1 expression. Data are shown as relative GSTZ1 expression / g liver or relative GSTZ1 expression / mg protein.
[b] Cytosolic yield was calculated based on the total cytosolic protein recovered experimentally. Mitochondrial yield was standardized to 30 mg mitochondrial protein per gram liver to correct for loss of mitochondria during differential centrifugation (Fleischer et al., 1979).
[c] Samples were dialyzed in 1.15% KCl, 0.05 M potassium phosphate buffer pH 7.4 before being assayed with 0.2 mM ^{14}C-DCA as substrate.
[d] Of the cytosol of four DCA rats, only two showed detectable activities. The limit of detection was 0.067 nmol/min/mg. Data are shown as mean ± S.D. N.D., not detectable.

Table 2-2. Characteristics of unique spectra of tryptic peptides of human and rat mitochondrial GSTZ1 identified by ESI-QTOF with 95% probability[a].

Peptide sequence[b]	Modifications identified by spectrum	Mascot ion score	Observed m/z	Actual peptide mass (AMU)	Spectrum charge	Actual minus calculated peptide mass (AMU)
Human						
41 DGGQQFSK 48		56.8	433.64	865.27	2	-0.12
49 DFQALNPMK 57	Oxidation (+16)	43.2	540.12	1,078.23	2	-0.28
207 QPDTPTELRA 216	Pyro-Glu[c] (-17)	49.0	555.71	1,109.39	2	-0.14
207 QPDTPTELRA 216		42.5	564.24	1,126.46	2	-0.10
Rat						
41 GGQQFSEEFQTLNPMK 57	Oxidation (+16)	37.9	657.87	1970.60	3	-0.27
134 AITSGFNALEK 144		57.1	575.73	1149.44	2	-0.16

[a] Probability score was calculated by Scaffold 2 software.
[b] Underlined amino acids were identified by MS with modifications.
[c] Pyroglutamate (Pyro-Glu) formed from cyclization of N-terminal glutamine.

Table 2-3. Michaelis-Menten parameters of the glutathione-dependent biotransformation of DCA in the dialyzed cytosol and mitochondria of rat livers.

	GSH[b]		DCA[c]	
	$^{App}K_m$ (mM)	$^{App}V_{max}$ (nmol/min/mg)	$^{App}K_m$ (mM)	$^{App}V_{max}$ (nmol/min/mg)
Rat mitochondria[a]	0.50 ± 0.12	0.56 ± 0.12	0.033 ± 0.002	0.57 ± 0.01
Rat cytosol[a]	0.19 ± 0.04**	1.67 ± 0.14	0.033 ± 0.005	1.66 ± 0.15

[a] Rat liver mitochondria and cytosol were dialyzed at 4°C overnight with three changes of 1.15% KCl, 0.05 M potassium phosphate buffer pH 7.4.
[b] With 0.2 mM DCA as substrate, cytosol was incubated with 0.05 – 2.5 mM GSH for 10 min and mitochondria were incubated with 0.1 – 7.5 mM GSH for 15 min.
[c] With DCA concentration range of 0.005 – 0.2 mM, cytosol was incubated with 2 mM GSH for 5 min and mitochondria were incubated with 5 mM GSH for 10 min.
** $p < 0.01$ compared to $^{App}K_m$ of mitochondria for GSH, analyzed by one-tailed t-test. Data are shown as mean ± S.D. of 3 rats.

CHAPTER 3
ROLES OF SUBJECT AGE AND HAPLOTYPE ON GSTZ1 EXPRESSION AND ACTIVITY WITH DICHLOROACETATE IN HUMAN LIVER

Specific Aim

Developmental changes and genetic polymorphisms of drug-metabolizing enzymes are respectively recognized as the major contributing factors to age-related and inter-individual differences in the pharmacotoxicology of many drugs. Several classes of GSTs (GSTA, GSTM, and GSTP) have been shown to exhibit distinct patterns of changes in their hepatic expression during human development (Strange et al., 1989). Studies using recombinant human GSTZ1 have revealed that the Z1A (KRT) variant possessed different kinetic properties and rates of inactivation with DCA as substrate and inhibitor, respectively, compared with other haplotypes. Given the observed differences in pharmacokinetics and toxicity between children and adults, and between Z1A and Z1D carriers and non-carriers, we investigated the role of subject age and haplotype in determining the hepatic expression and activity of GSTZ1 in human liver cytosol samples ranging from 10 weeks of gestation to 74 years of life.

Materials and Methods

Human Liver Samples

A total of 249 human liver samples ranging from 10 weeks of gestation to 74 years of life were used in the current study. Human liver cytosol including 61 pre-natal samples and 167 post-natal samples was obtained from a liver bank at the Medical College of Wisconsin (Milwaukee, WI). Donor characteristics and subcellular fraction preparations have been described previously (Koukouritaki et al., 2002). The other 21 post-natal samples were de-identified human livers, of which 14 were obtained from Vanderbilt University (Nashville, TN) and 7 were collected during surgery at Shands

Hospital at University of Florida (Gainesville, FL). Liver cytosol and mitochondria of these samples was prepared and dialyzed exactly as described in Chapter 2. The pellet of cell nuclei was used to isolate DNA for genotyping and haplotype analysis. Protein concentration was determined by BCA Protein Assay (Thermo Fisher Scientific, Waltham, MA).

GSTZ1 Activity with DCA

The specific activity of GSTZ1 was measured with [1-^{14}C]DCA as substrate and assay products were analyzed by HPLC coupled-radioactivity flow detector as previously described (James et al., 1997). Stock [1-^{14}C]DCA (55 mCi/mmol with 99% purity; American Radiolabeled Chemicals, Inc., St. Louis, MO) was converted to the sodium salt by addition of $NaHCO_3$ and diluted with unlabeled DCA (TCI America, Portland, OR). Human liver cytosol, 0.2 to 0.6 mg, was incubated with 1 mM glutathione, 0.1 M Hepes-NaOH pH 7.6 and a saturating concentration of DCA at 0.2 mM in an assay volume of 0.1 ml. The reaction was started by adding DCA, allowed to proceed for 15 min at 37°C with gentle shaking and stopped by adding 0.1 ml ice-cold methanol. All assays were performed in duplicates; substrate consumption did not exceed 15%. The specific activity of GSTZ1 was expressed as nmol glyoxylate formed/min/mg protein. The limit of detection (LOD) was 0.0147 nmol/min/mg. Samples with activity below LOD were imputed a value equal to the LOD divided by the square root of 2, i.e. 0.010 nmol/min/mg.

Western Blot Analysis of GSTZ1 Expression

Known amounts of protein (5 to 60 μg) were separated on 4-15% SDS-PAGEs (Tris-HCl Gel; Bio-Rad Laboratories, Hercules, CA) and subsequently electrotransferred onto polyvinylidene fluoride membrane (Millipore Corporation, Billerica, MA). The

amount of cytosol used was guided by GSTZ1 activity found in DCA assay. After blocking, the membrane was incubated with rabbit polyclonal anti-hGSTZ1C-1C 1:5000 (Cocalico Biologicals, Inc., Reamstown, PA) then with horseradish peroxidase-conjugated donkey anti-rabbit IgG 1:2000 (GE Healthcare, Piscataway, NJ). Protein signal was developed by ECL Plus Western Blotting detection reagents (Thermo Fisher Scientific) on Amersham Hyperfilm ECL (GE Healthcare). Films were digitized by scanning and the density of bands was analyzed by QuantiScan Software (Biosoft, Cambridge, UK). A GSTZ1 standard curve was constructed using 0.55-17.6 ng of purified recombinant hGSTZ1C-1C (Guo et al., 2006). A designated human liver cytosol, 5 µg, was used as a reference control on each blot. The signal of each individual test sample was normalized against the reference control for analysis. The GSTZ1 content of samples was calculated by fitting data to the GSTZ1 standard curve and expressed as µg GSTZ1 per mg cytosolic or mitochondrial protein. Data were analyzed using Microsoft Office Excel 2007. The LOD was 0.0092 µg GSTZ1/mg protein. Samples with expression below LOD were imputed a value equal to the LOD divided by the square root of 2, i.e. 0.0065 ng GSTZ1/µg protein.

Genotyping

DNA from selected liver samples was subjected to PCR followed by pyrosequencing (Langaee and Ronaghi, 2005), targeting the three known GSTZ1 non-synonymous single nucleotide polymorphisms (SNPs): G94>A, Glu→Lys at amino acid position 32; G124>A, Gly→Arg at position 42; and C245>T, Thr→Met at position 82. Genotyping analysis was carried out using a PSQ HS 96 System (Biotage, Uppsala, Sweden). Haplotypes were inferred from the unphased data by computational methods (PHASE software version 2.0.2) (Stephens et al., 2001).

Data Analysis

Age breakpoints were determined by results obtained from regression tree analysis that gave the least deviation within groups and maximum variance between groups (CART v6, Salford Systems, San Diego, CA). Outliers were defined as having specific contents 1.5-fold interquartile range away from the lower or upper quartiles. Statistical comparisons between age groups were performed using Kruskal-Wallis nonparametric test, followed by stepwise step-down comparisons (IBM SPSS Statistics 19, Chicago, IL). A p value < 0.05 was accepted as significant. Data analyses and Loess curve fit were performed on IBM SPSS Statistics 19. Correlation analysis between GSTZ1 activity and expression included samples with specific contents above the LODs and was determined using Pearson's correlation (GraphPad Prism v4.03, San Diego, CA).

Results

Developmental Pattern of GSTZ1 in Human Liver Cytosol

To quantitate GSTZ1 protein expression, we compared GSTZ1 immunoreactivity in individual liver cytosol to a standard curve constructed with purified recombinant hGSTZ1C (Figure 3-1). The activity of GSTZ1 was evaluated using the probe substrate DCA at a saturating concentration of 0.2 mM. Overall, GSTZ1 protein expression increased with age after birth and was paralleled by the increase in its activity with DCA (Figure 3-2). Scatter plot analyses assisted with Loess curve fitting (not shown) suggested four phases of GSTZ1 development: 1) undetectable or very low levels in the fetus; 2) a rapid rise after birth to near half of adult levels by age 1; 3) the increase continued gradually over the course of children development; and 4) GSTZ1 expression

and activity were sustained at a stable level from late adolescence to age 74, the oldest sample studied.

During pregnancy, fetal liver exhibited undetectable to very low levels of cytosolic GSTZ1 expression (<0.05 µg GSTZ1/mg protein) and activity (<0.1 nmol glyoxylate/min/mg). A slight increase was shown for GSTZ1 activity from 2nd trimester (13 – 28 wk gestation) to 3rd trimester (28 – 40 wk) (median 0.023 nmol/min/mg, n = 37 vs 0.042 nmol/min/mg, n = 11; p = 0.012, Mann-Whitney U test) but not for expression.

GSTZ1 developmental changes between age groups were quantitated by dividing samples into 5 age brackets based on results of regression tree analysis. Steady and significant increases in both GSTZ1 protein expression (Figure 3-3A) and DCA-metabolizing activity (Figure 3-3B) were observed from prenatal samples to samples of >7 – 74 Y. In particular, a 3-fold increase in mean values was shown from the age bracket of >0 -1 M to >1M – 1Y. Less than 2-fold increases were shown from >1M - 1Y to >1 - 7Y and from >1 – 7Y to >7 - 74Y. Comparison of samples between older children (>7 – 21Y) and adults (>21 – 74Y) showed no further change with age for either expression or activity.

Impact of Z1A Variant

Several outliers were observed in the box and whisker plot analyses of GSTZ1 expression and activity. Of particular interest, 6 out of the 7 activity outliers in the >7Y – 74Y bracket carried one allele of Z1A (Figure 3-3B). Plotting all known Z1A carriers in the scatter plots demonstrated a major impact of this allele on possessing high DCA-metabolizing activity but not protein expression, especially in samples aged 7 and above (Figure 3-2). No specificity was observed for the outliers of GSTZ1 expression.

Correlation Analysis of GSTZ1 Activity and Expression

A fair correlation of $r^2 = 0.51$ was obtained between GSTZ1 expression and activity with DCA when all postnatal samples with specific contents above the LODs were analyzed. However, a few individuals clearly segregated from the main body by exhibiting 2- to 3-fold higher activity with DCA than others at similar levels of expression (Figure 3-4). In accord with the observed impact of the Z1A variant, those high activity individuals carried at least one allele of Z1A. Subsequent grouping of the genotyped individuals into Z1A carriers or noncarriers improved the correlations to $r^2 = 0.90$ and 0.68, respectively. Therefore, GSTZ1 activity with DCA is dependent on both the level of protein expression and the haplotype of GSTZ1.

Role of Haplotype on GSTZ1 Expression and Activity

We further analyzed the role of each haplotype in determining GSTZ1 activity and expression. Individuals carrying only Z1C (EGT) and/or Z1B (KGT) alleles were grouped together due to their lack of difference in activity or expression (analysis not shown). Z1A (KRT) carrier, Z1D (EGM) carrier and Z1A/Z1D heterozygote were grouped separately due to a recent study indicating low in vivo activity by carriers of Z1D and Z1A alleles (Shroads et al., 2011) and the current study showing high in vitro activity by Z1A allele.

In liver cytosol of individuals aged 3 to 74, GSTZ1 haplotype had no effect on protein expression as shown by the similar medians of different haplotype groups (Figure 3-5A). On the other hand, Z1A allele when paired with Z1C allele clearly conferred a larger ratio of GSTZ1 activity to expression compared to other alleles, demonstrating higher DCA-metabolizing activity at a given level of protein expression (Figure 3-5B). Two samples in our liver bank were homozygous for Z1A, however, both

were aged less than 1 M. These two 1A/1A homozygotes, like 1C/1A heterozygotes, also exhibited relatively large ratios of activity to expression (ratio = 2.9 and 3.8).

The two 1D/1A heterozygotes, although having similar ratios of activity to expression, exhibited distinct levels of expression: one was near the medians of other haplotypes and the other was expressed at a very low level. In addition to the low expression 1D/1A heterozygote, two individuals of 1B/1B and 1B/1C haplotype also possessed very low GSTZ1 content for their ages (5 – 11 Y) (Figure 3-5A). A rare haplotype, KRT/KGT, was identified in an individual of 17 days old. This individual, however, had essentially no expression nor activity of GSTZ1 in that GSTZ1 immunoreactivity was invisible on its Western blot and the activity in assay was identical to blank, neither of which changed by assaying increased amounts of protein. Resequencing the *GSTZ1* gene of these individuals for the newly identified V99M SNP, however, did not find the mutation.

Role of Haplotype on Mitochondrial GSTZ1

In Chapter 2, we reported the presence of GSTZ1 in liver mitochondria. Examination of GSTZ1 expression in cytosol and mitochondria showed similar distribution of the enzyme between the two compartments, independent of the allelic differences (Table 3-1). As with cytosolic GSTZ1, mitochondrial GSTZ1 of 1A/1C variant exhibited ~3-fold higher activity with DCA than Z1A noncarriers at a given level of expression. Therefore, haplotype influenced mitochondrial and cytosolic GSTZ1 similarly for DCA-metabolizing activity, but had no effect on protein expression or subcellular distribution of the enzyme.

Discussion

By studying human liver cytosols from 10 weeks of gestation to 74 years of life, we demonstrated age as the major determinant of GSTZ1 protein expression and activity with DCA during human liver development. Similar to many of the DMEs studied to date, GSTZ1 was minimally expressed in the fetus and started increasing in the neonatal period. The neonatal onset of GSTZ1 expression was also observed in the mRNA level in mouse livers, which reached adult level just 10 days after birth (Cui et al., 2010). Both transcriptional activation by members of the proline and acidic amino acid rich (PAR) family and epigenetic regulation of DNA and histone have been suggested to contribute to the postnatal onset of DMEs (Hines, 2008). Indeed, postnatal enrichment of histone H3 lysine-4 dimethylation has been shown in mouse *Gstz1* gene (Cui et al., 2010).

GSTZ1 haplotype had no effect on protein expression or subcellular distribution of the enzyme, but had a major impact on enzymatic activity with DCA. Consistent to results obtained with the polymorphic variants of recombinant hGSTZ1 (Blackburn et al., 2001), the Z1A allele, paired with or without the Z1C allele, conferred higher DCA-metabolizing activity for a given level of expression in human liver samples. However, it was inconclusive whether the effect of the Z1A allele was dominant over or additive with the Z1C allele due to small number of samples. For the same reason, it remained unknown if Z1A conferred a similar effect on activity when paired with the Z1D allele, or rendered the enzyme unstable by the rare allelic combination. It is also noteworthy that although the Z1A allele-associated high ratio of activity/expression was observed in individuals as early as 20 days postnatal, its impact in the population was not prominent

until adolescence. This either fits into the convention of "growing into the phenotype", or, is a result of low levels of protein expression in young KRT carriers.

Unexplained by the current knowledge on GSTZ1 polymorphism, several individuals in our liver bank exhibited very low GSTZ1 expression and activity for their ages. A novel Val99Met SNP was recently identified in a KGM/KGT individual with extraordinarily slow rate of DCA clearance (Shroads et al., 2011). However, none of the individuals with low GSTZ1 function in our study carried this mutation. Leu8Pro is another less studied SNP that was suggested to be very poorly expressed (Blackburn et al., 2001), but its occurrence has not yet been reported in the population. Therefore, it may be of interest to investigate the possible roles of L8P as well as other genetic or environmental factors that may contribute to the low functionality of GSTZ1.

Human pharmacokinetics of DCA has been shown with age- and GSTZ1 haplotype-dependent differences (Shroads et al., 2008; Shroads et al., 2011). The current finding of older children and adults (7 – 74 Y) having higher GSTZ1 activity than young children (1 – 7 Y), however, does not explain the slower clearance of DCA in adults after chronic treatment (see Table 1-2) (Shroads et al., 2008). On the other hand, Z1A allele-associated higher activity with DCA is consistent with the faster drug clearance by Z1A carriers after the 1st DCA dose (see Table 1-3) (Shroads et al., 2011). No evidence of low GSTZ1 function was observed for Z1D allele. Thus, the current study provided no explanation for the greater reduction in DCA clearance in Z1A/Z1A and Z1A/Z1D individuals after repeated doses. We speculate that this altered effect of Z1A allele in clearance between the initial and repeated doses may be related to a haplotype-dependent susceptibility to DCA inactivation (see Chapter 4). Similarly, the

apparent lack of correlation between age-related decrease in DCA clearance and increase in GSTZ1 activity may be related to DCA-induced inactivation of GSTZ1 rather than the initial enzymatic activity.

GSTZ1/MAAI has the important physiological function of isomerizing maleylacetoacetate at the penultimate step of phenylalanine/tyrosine catabolism. In the fetal liver, this pathway is rate limited by tyrosine aminotransferase that has been shown to possess very low activity in the fetus and increase rapidly after birth (Delvalle and Greengard, 1977; Andersson et al., 1980; Ohisalo et al., 1982). Therefore, in fetal liver maleylacetoacetate presumably exists at a low concentration, so that nonenzymatic conversion to fumarylacetoacetate could be sufficient for its degradation (Fernandez-Canon et al., 2002). As with tyrosine aminotransferase, the rapid onset of GSTZ1/MAAI in neonates may be regarded as a coordinated and adaptive response to the increased intake and thus degradation of amino acids as required for infant growth.

In conclusion, we reported a neonatal onset and an age-related increase in GSTZ1 protein expression during human liver development. GSTZ1 activity with DCA is directly correlated to the level of protein expression and dependent on GSTZ1 haplotype. The GSTZ1A (KRT) allele, paired with or without the Z1C allele, confers a ~3-fold higher activity with DCA at a given level of protein expression than other haplotypes that possess similar activities with DCA.

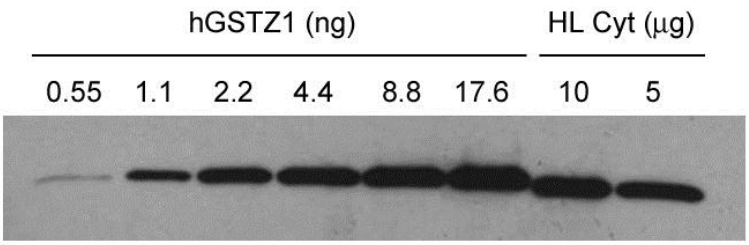

A

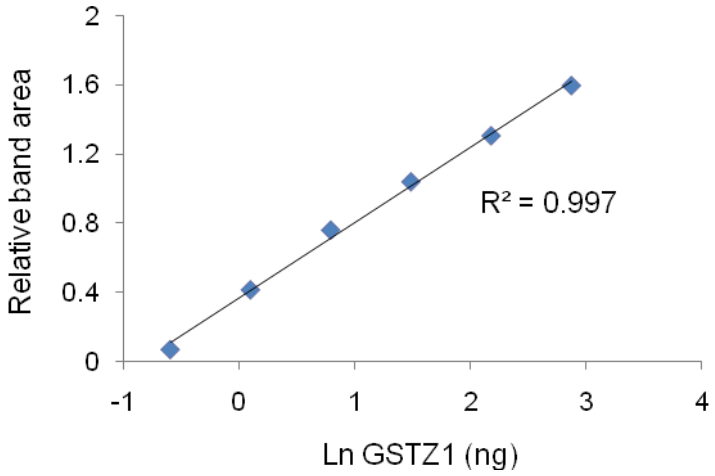

B

Figure 3-1. Western blot analysis of GSTZ1 in 0.55 – 17.6 ng purified hGSTZ1C-1C and 5 and 10 µg of one human liver cytosol (HL cyt). A) Western blot. B) Standard curve of 0.55 – 17.6 ng GSTZ1 expression analyzed by linear regression.

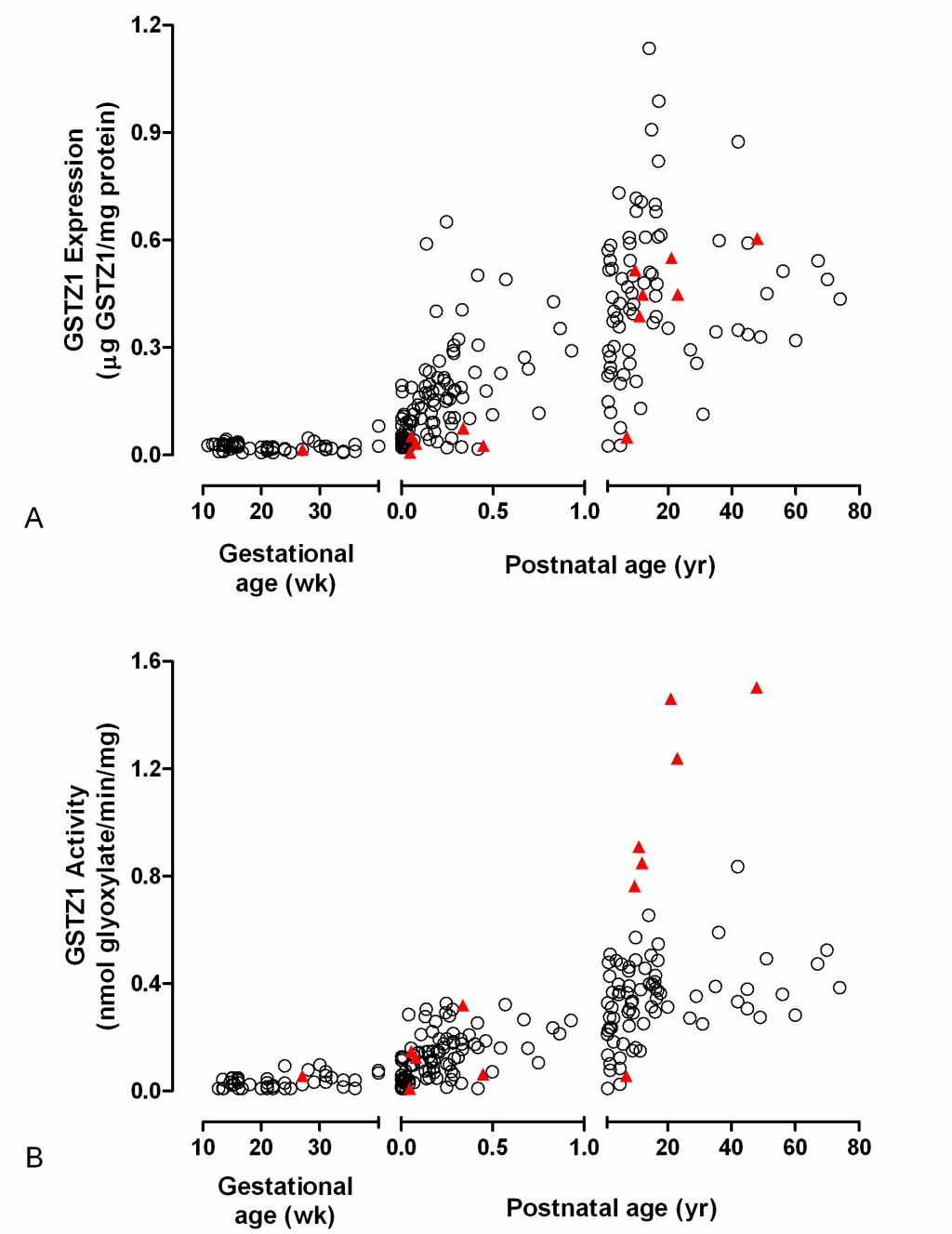

Figure 3-2. Scatter plot analyses of GSTZ1 A) protein expression and B) activity with DCA as a function of age. Axis breaks are set at birth and 1 year. Age of prenatal samples is shown as gestational age. Samples from individuals that carried at least one allele of GSTZ1A (KRT) are shown as filled triangle (▲) and all the others are shown as open circle (○).

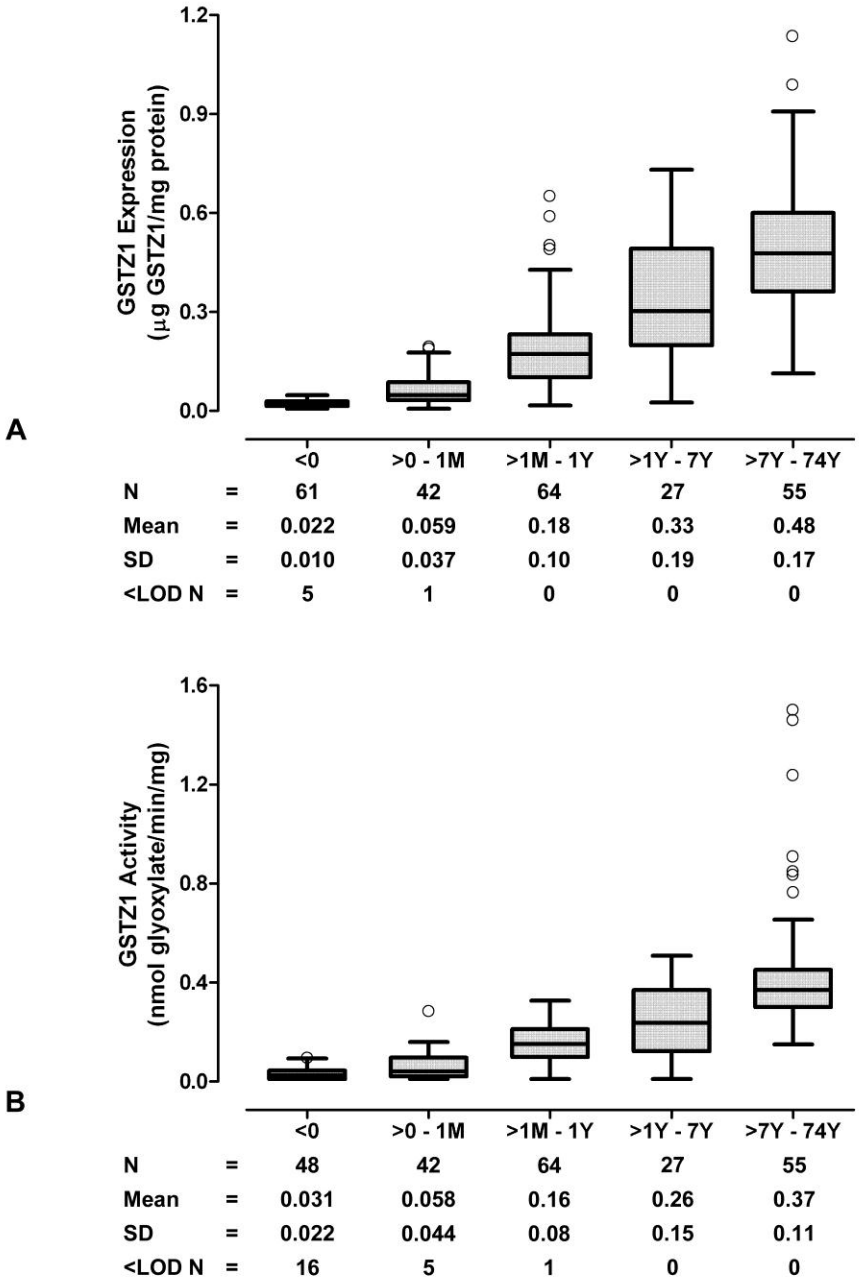

Figure 3-3. Box and whisker plot analyses of GSTZ1 A) protein expression and B) activity with DCA as a function of age groups. The horizontal bar, box and whiskers denote the median, interquartile range and the lowest to highest values of the group, respectively. Outliers (○) were defined as having specific contents 1.5-fold interquartile range away from the lower or upper quartiles. Mean and SD were reported and outliers were excluded from the analyses. Statistical significances ($p < 0.05$) were obtained between age groups as analyzed by Kruskal-Wallis nonparametric test, followed by stepwise step-down test. The number of samples having specific contents below the LODs was reported (<LOD N). M, month; Y, year.

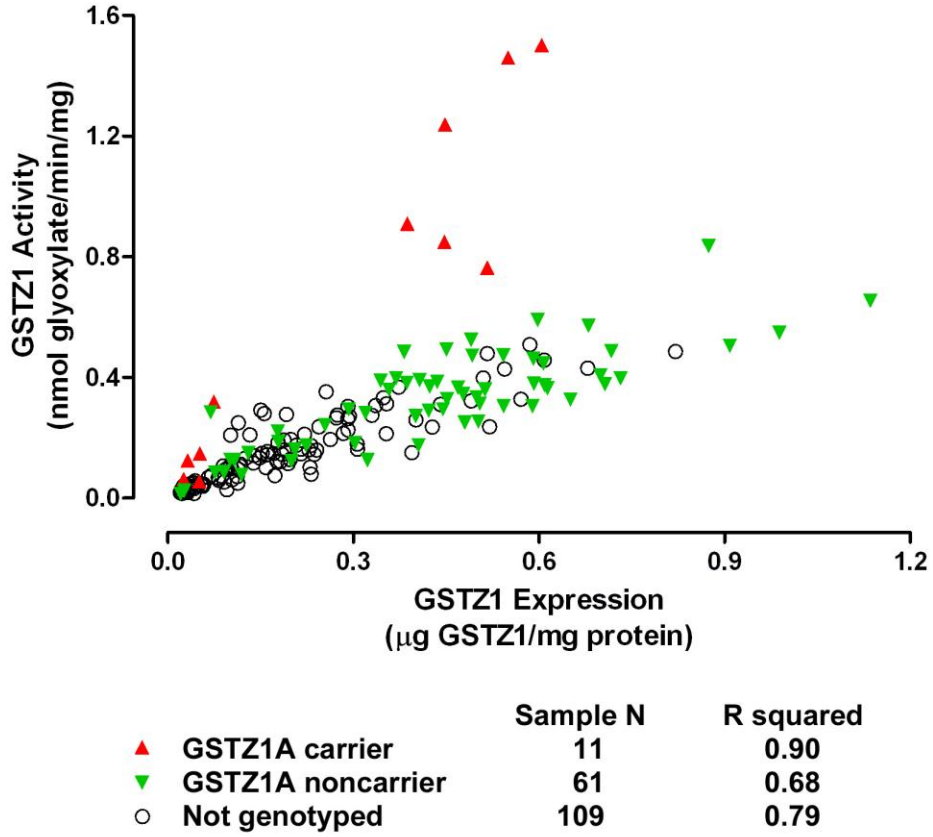

Figure 3-4. Correlation analysis of GSTZ1 protein expression and activity with DCA. R squared values were determined by Pearson correlation. The correlations were significant for all four groups ($p < 0.0001$). Postnatal samples with both activity and expression above the LODs were included in the analysis. Most samples above and selective sample below age 3 were genotyped for GSTZ1.

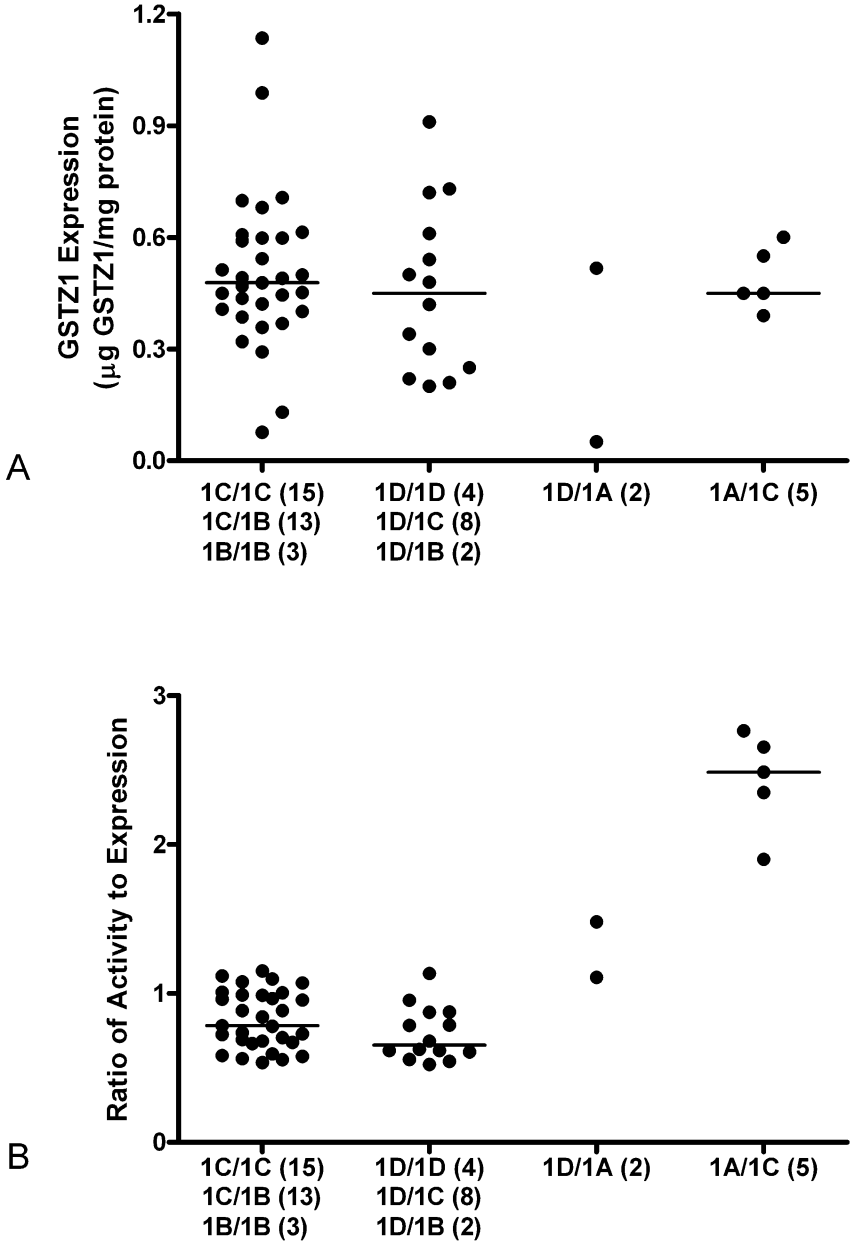

Figure 3-5. Role of GSTZ1 haplotype on A) protein expression and B) the ratio of DCA-metabolizing activity to protein expression. Samples of age 3 and above with expression and activity above the LODs were included in the analysis. The number of samples of each haplotype is given in parenthesis. The horizontal bar denotes the median.

Table 3-1. GSTZ1 expression and activity with DCA in cytosol and mitochondria of individuals with various haplotypes.

	Age (year)	GSTZ1 Haplotype	Cytosol			Mitochondria		
			Activity	Expression	Ratio of Act to Exp	Activity	Expression	Ratio of Act to Exp
			nmol/min/mg	µg GSTZ1/ mg cytosol		nmol/min/mg	µg GSTZ1/mg mitochondria	
HL735	74	1C/1C	0.39	0.44	0.88	0.14	0.20	0.69
HL733	70	1C/1B	0.53	0.49	1.07	0.21	0.19	1.09
HL750	10	1C/1B	0.57	0.68	0.84	0.30	0.27	1.11
HL20	67	1D/1D	0.47	0.54	0.87	0.16	0.24	0.67
Mean ± SD (n=4)					0.92 ± 0.10			0.89 ± 0.24
HL10	23	1C/1A	1.24	0.45	2.76	0.87	0.30	2.87
HL97	21	1C/1A	1.46	0.55	2.65	0.46	0.22	2.11
HL742	48	1C/1A	1.50	0.60	2.49	0.51	0.24	2.17
Mean ± SD (n=3)					2.63 ± 0.14			2.38 ± 0.42

CHAPTER 4
CHLORIDE MODULATES GSTZ1 HAPLOTYPE-DEPENDENT INACTIVATION BY DICHLOROACETATE

Specific Aim

To date, four major polymorphic variants of GSTZ1, i.e., EGT, KGT, EGM and KRT, have been studied in some detail both in vitro and in vivo. Study of recombinant enzymes showed that the KRT variant possessed 4-5-fold higher specific activity with DCA as substrate and 2-fold slower rate of inactivation by DCA compared to the other variants, which grouped together for activity and rate of inactivation (Tzeng et al., 2000; Blackburn et al., 2001). That the KRT allele-conferred higher activity with DCA was confirmed with human liver samples by our work (Chapter 3). Nevertheless, pharmacokinetic studies showed that KRT/KRT and KRT/EGM individuals exhibited a greater reduction in DCA clearance after repeated doses compared to EGT carriers (Shroads et al., 2011). Our previous study (Cornett et al., 1999) failed to reproduce Tzeng et al.'s (2000) result of DCA inactivation of human cytosolic GSTZ1 in vitro, which we speculate to be a result of the presence of chloride in our samples. To investigate these discrepancies, we used human liver cytosols of different GSTZ1 haplotypes to examine 1) DCA-induced inactivation of GSTZ1 and 2) the role of chloride in modulating GSTZ1 activity.

Materials and Methods

Human Liver Samples and GSTZ1 Genotype Information

De-identified human livers homozygous for EGT and EGM, and heterozygous of EGT/KRT were used in the current study. The sources of the livers and GSTZ1 genotyping procedures are described in Materials and Methods section of Chapter 3.

Assay of DCA-Induced Inactivation of GSTZ1 in Human Liver Cytosol

Human liver cytosol was isolated exactly as described in Chapter 2. Aliquots of cytosol were dialyzed against 0.1 M potassium phosphate pH 7.4 using Slide-A-Lyzer® Dialysis cassette (10kD MWCO; Thermo Fisher Scientific) with three changes of buffer to ensure complete removal of small molecules. DCA-induced inactivation of GSTZ1 was assayed by adapting the method of Tzeng et al (2000). In the presence or absence of KCl or other salts, dialyzed cytosol (0.6 mg/ml) was incubated with 0.5 mM unlabelled DCA, 5 mM glutathione and 0.1 M potassium phosphate in an assay volume of 500 µl at 37°C for 2 h. To determine the EC50 of chloride in protecting GSTZ1 from DCA inactivation, samples were incubated with 0.77 – 308 mM KCl; the effects of other anions as their sodium or potassium salts were tested at a concentration of 38 mM in assays; control incubations lacked DCA or additive salts. To study the time course of GSTZ1 inactivation, assay mixtures were incubated for 0 – 14 h with 38.3 mM KCl or 0 – 90 min without KCl. At the end of incubation, unbound substrate and product were removed by ultrafiltration through Amicon Ultra – 0.5 ml filters of 10 kD MWCO (Millipore Corporation) following 3 concentration-dilution cycles with 0.1 M potassium phosphate pH 7.4. Protein recovered by the filter was assayed for concentration and then activity with 0.2 mM [^{14}C]DCA as described in Chapter 3. Protein concentration was determined using Bio-Rad Protein Assay (Bio-Rad Laboratories) with bovine serum albumin (Sigma-Aldrich) as protein standard.

Data Analysis

To determine the EC50 of chloride in protecting GSTZ1 from DCA inactivation, assay activity was normalized as a percent of control and plotted against the log KCl concentration. EC50 was obtained by fitting the data to a dose-response sigmoidal

curve with the top constrained to 100% and the bottom to 0%. To determine the inactivation half-life ($t_{1/2}$) of GSTZ1, the natural log of assay activity (A) divided by control activity (A_0, tubes assayed at time 0) was plotted against incubation time. Linear regression analysis was performed to fit data to the equation $\ln(A/A_0) = - k_{obs}t$ with lines forced to go through (0, 0). The inactivation $t_{1/2}$ was determined from the equation $t_{1/2} = \ln 2/k_{obs}$. Data analysis was performed on GraphPad Prism v4.03 (San Diego, CA). Student's *t* test was performed on Microsoft Office Excel 2007.

Results

Chloride Protected GSTZ1 from DCA Inactivation

In an attempt to reproduce Tzeng et al.'s (2000) result of in vitro inactivation of GSTZ1 by DCA, we conducted several preliminary experiments and identified chloride to be a modulating factor. Chloride protected human cytosolic GSTZ1 from DCA-induced inactivation in a chloride concentration- and GSTZ1 haplotype-dependent manner (Figure 4-1). To achieve 50% protection of GSTZ1 from DCA inactivation, a significantly higher (2.5X) concentration of chloride was required for EGT/KRT individuals (EC50 33.6 ± 2.3 mM; mean ± SD, n=3), compared to EGT/EGT (12.3 ± 2.7 mM, n =3) and EGM/EGM (13.8 mM, n=1) individuals (Table 4-1). Chloride is reported to be present at 38.3 mM in human livers (Widdowson and Dickerson, 1960). At 38 mM chloride, EGT/KRT individuals were inactivated to a larger extent than other variants after 2 h incubation.

Time Course of GSTZ1 Inactivation by DCA

We next examined the time course of cytosolic GSTZ1 inactivation by 0.5 mM DCA in the absence or presence of physiological concentration (38 mM) of chloride (Figure 4-2). In the absence of chloride, DCA rapidly reduced GSTZ1 activity to 50% of

control level within 30 min for all individuals, with a slightly longer $t_{1/2}$ in EGT homozyotes (Table 4-2). With addition of 38 mM chloride, however, the rate of GSTZ1 inactivation by DCA was substantially reduced. Furthermore, a 2-fold difference in GSTZ1 inactivation $t_{1/2}$ was observed between KRT carriers and non-carriers: over 5 h for EGT and EGM homozygotes and 2.5 h for EGT/KRT heterozygotes.

Effects of Other Anions

We further screened some other anions for their influence on DCA-induced inactivation of GSTZ1 by using a salt concentration of 38 mM over a 2 h incubation (Table 4-3). Of the halide series, Br^- and I^- exhibited a more potent protection for GSTZ1 than Cl^-, while F^- had no apparent effect. Among other anions tested, only SO_3^{2-} showed protection for GSTZ1 with a potency stronger than that of Cl^-.

Discussion

The current study showed that the rate of DCA-induced inactivation of GSTZ1 was dependent on GSTZ1 haplotype and the presence of certain anions, such as chloride, bromide, iodide and sulfite. Chloride, a major physiological electrolyte, dose-dependently attenuated DCA-induced inactivation of GSTZ1. At a normal liver concentration of chloride (38 mM), cytosolic GSTZ1 of EGT/KRT individuals was inactivated > 2X faster by DCA than that of EGM and EGT homozygotes.

The finding of chloride protection explains Cornett et al.'s (1999) failure to observe DCA inactivation in human liver cytosol. In that study, cytosols of EGT homozygotes were dialyzed in a buffer containing 1.15% KCl, which resulted in ~30 mM chloride in assay and effectively prevented GSTZ1 inactivation after an incubation of 30 min.

Contradictory to the knowledge gained from the recombinant enzymes (Tzeng et al., 2000), the human cytosolic form of the KRT variant was more susceptible to DCA

inactivation, regardless the presence of chloride. Meanwhile, it is noteworthy that the recombinant enzymes were stored in a chloride-containing buffer. Although the exact reason for this discrepancy is unknown, we suspect various factors contribute, including inconsistent concentrations of chloride in assays and structural variation in the N terminus where the recombinant enzyme was constructed with the His-tag near the GSH-binding site.

KRT variant differs from other variants by the mutation of Gly to Arg at residue 42, which is located at a loop area on the top of GSH-binding site. This loop region was suggested to be highly mobile and function as a gateway to the binding site of the enzyme. Therefore, conformational changes in the loop region were previously proposed to occur upon uptake or release of substrate and/or product, and between variants carrying Gly or Arg (Blackburn et al., 2001). Given that Arg has a long and positively charged side chain, it may also exhibit ionic interactions with the negatively charged substrate (DCA), product (glyoxylate) and/or currently identified modulating anions (halides and sulfite) that do not apply to the variants with Gly at position 42.

In addition to chloride, some other anions (Br^-, I^- and SO_3^{2-}) showed similar protective effects for GSTZ1. On the other hand, sulfate ion (SO_4^{2-}), which co-crystallized with the KRT variant of the recombinant hGSTZ1 in the proposed active site (Polekhina et al., 2001), afforded no protection in the current study. We speculate that either the active site or an allosteric site of GSTZ1 may be involved in the binding of anions. Depending on the property of the anion and its interaction with GSTZ1 and/or DCA, the anion binding may trigger conformational change and thus modulate the interaction between DCA and the GSTZ1 enzyme. Interestingly, Tzeng et al. (2000) also

noted some protective effect by N-acetyl-L-cysteine but not KCN. The mechanism of action they proposed was that N-acetyl-L-cysteine blocked the electrophilic intermediate of DCA from attacking GSTZ1. However, this mechanism is unlikely to explain the protection afforded by halides or sulfite.

Analyses of previous studies suggest that chloride protection applies to rat GSTZ1 and has pharmacological significance. The inactivation $t_{1/2}$ of rat GSTZ1 by 0.5 mM DCA increased from 5 min in chloride-free cytosol of Fisher 344 rats (Tzeng et al., 2000) to about 30 min in chloride-containing cytosol of S-D rats (Cornett et al., 1999). I.p. injection of 0.3 mmol (i.e. 45 mg) of DCA/kg to Fisher 344 rats reduced the activity and expression of liver cytosolic GSTZ1 to 50-60% of control levels 1.5 h after treatment (Anderson et al., 1999). Since DCA is rapidly distributed to the liver after i.p. injection, the hepatic GSTZ1 should have been reduced more rapidly if not for the protection of modulating factors, such as Cl^- and other anions.

Chloride is known to be present at 38.3 mM in the liver of adults and slightly higher in infants (4-7 months old; 42.8 mM) and newborns (55.8 mM) (Widdowson and Dickerson, 1960). Although little is known about the concentrations of other anions in the liver, bromide and iodide have been detected at ~26 µM and ~ 0.34 µM, respectively, in the human whole blood (Zhang et al., 2010) and sulfite at ~1.2 µM in the serum (Mitsuhashi et al., 2004). Additionally, sulfite was reported to reduce oxalate production from glyoxylate in vitro and from rats i.v. infused with DCA (Sharma and Schwille, 1993). Together, current results strongly suggest that chloride and perhaps other anions protect GSTZ1 from in vivo inactivation by DCA and may therefore be a factor modulating the rate of DCA clearance after repeated doses.

In conclusion, we demonstrated that chloride attenuated DCA-induced inactivation of GSTZ1 in a chloride concentration- and GSTZ1 haplotype-dependent manner. In contrast to results obtained with the recombinant enzyme, the human cytosolic form of the KRT variant was more rapidly inactivated by DCA. At a physiological concentration of chloride and 0.5 mM DCA, GSTZ1 inactivation $t_{1/2}$ was 2-3 h shorter for KRT/EGT individuals than EGT and EGM homozygous individuals. This may contribute to the greater reduction in DCA clearance observed in KRT/KRT and KRT/EGM individuals after repeated doses.

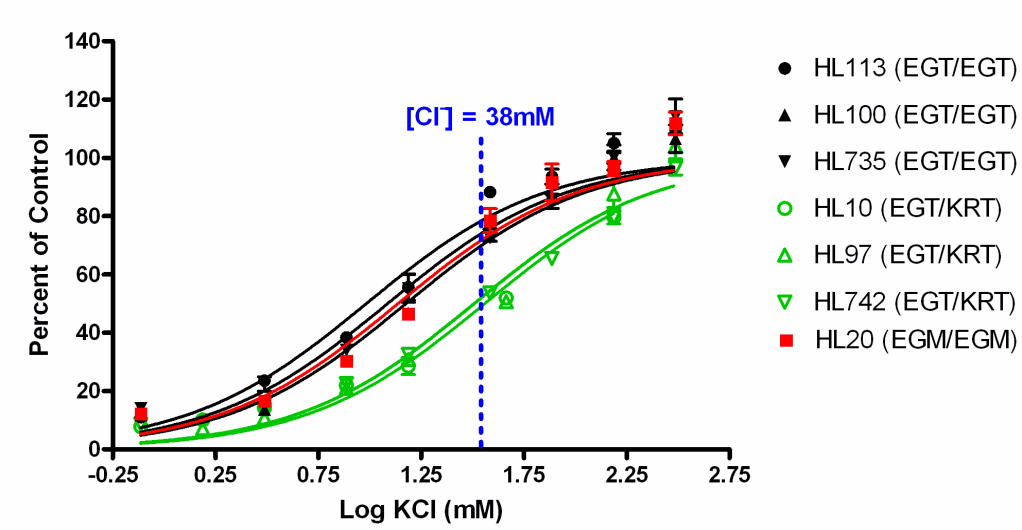

Figure 4-1. Chloride protected human liver cytosolic GSTZ1 from DCA inactivation in a [Cl⁻]- and GSTZ1 haplotype-dependent manner. Dialyzed human liver cytosol, 0.6 mg/ml, was incubated with 0.5 mM DCA, 5 mM GSH and 0.77 – 308 mM KCl in 0.1 M K-phosphate buffer pH 7.4 at 37°C for 2 h. Data were analyzed as described in Materials and Methods. The control activity and EC50 of chloride protection for each sample were summarized in Table 4-1.

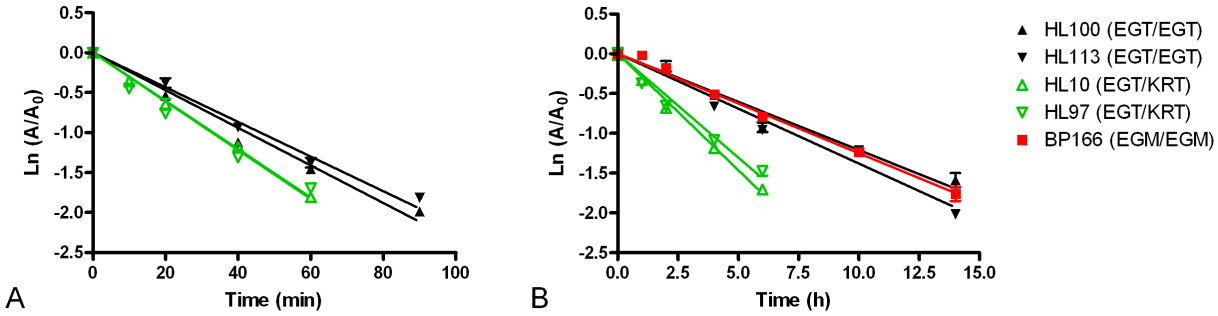

Figure 4-2. The time course of GSTZ1 inactivation by DCA in the A) absence and B) presence of 38 mM KCl. Human liver cytosol, 0.6 mg/ml, was incubated with 0.5 mM DCA, 5 mM GSH in 0.1 M K-phosphate buffer pH 7.4 with or without 38.3 mM KCl at 37°C for the indicated period of time. The inactivation $t_{1/2}$ of GSTZ1 was determined as described in Materials and Methods, and summarized in Table 4-2.

Table 4-1. Summary of GSTZ1 control activity with DCA and chloride concentration to achieve 50% protection of GSTZ1 from DCA inactivation (EC50) obtained from Figure 4-1.

EGT/EGT			EGT/KRT			EGM/EGM		
ID	Control activity nmol/min/mg	EC50 mM	ID	Control activity nmol/min/mg	EC50 mM	ID	Control activity nmol/min/mg	EC50 mM
HL100	0.61	15.0	HL10	0.85	36.3	HL20	0.35	13.8
HL113	0.73	9.6	HL97	1.27	32.2			
HL735	0.29	12.2	HL742	1.06	32.3			
Mean ± SD (n=3)		12.3 ± 2.7			33.6 ± 2.3***			

***, $p < 0.005$ compared to EC50 of EGT/EGT individuals, analyzed by two-tailed *t* test assuming equal variances.

Table 4-2. Summary of GSTZ1 inactivation half-lives ($t_{1/2}$) obtained from Figure 4-2.

	Inactivation $t_{1/2}$ (h)	
GSTZ1 Haplotype	without Cl^-	with Cl^-
EGT/EGT (n=2)	0.53, 0.49	5.02, 5.73
EGT/KRT (n=2)	0.39, 0.38	2.37, 2.67
EGM/EGM (n=1)	Not determined	5.55

Table 4-3. Effects of various anions in modulating GSTZ1 inactivation by DCA. Sodium or potassium salt of various anions at 38 mM was incubated with HL113 (EGT/EGT) liver cytosol, 0.5 mM DCA and 5 mM GSH at 37^{o}C for 2hr. Activity was shown as a percent of control, which was preincubated without DCA or additive salts.

	DCA only	F^-	Cl^-	Br^-	I^-	SO_4^{2-}	SO_3^{2-}	CO_3^{2-}	CN^-
% of control	12%	13%	80%	105%	102%	15%	100%	9%	3%

CHAPTER 5
CONCLUSION

In this dissertation, we studied the roles of mitochondrion, subject age, enzyme haplotype and chloride interaction in GSTZ1-catalyzed biotransformation of DCA. Mitochondrion, the principal site of DCA's pharmacological action, is a second site of DCA biotransformation. The reaction is catalyzed by a mitochondrial pool of GSTZ1 localized in the matrix. The identity of mitochondrial GSTZ1 was confirmed by partial protein sequences obtained from LC-MS/MS analysis. Similar to the cytosolic form, mitochondrial GSTZ1 possessed catalytic activity with DCA and was inactivated by DCA treatment. With DCA as substrate, rat mitochondrial GSTZ1 exhibited a higher apparent K_m for GSH than cytosolic GSTZ1, suggesting possible modification of the mitochondrial form relative to the cytosolic form. GSTZ1 haplotype had no effect on the relative distribution of the enzyme between cytosol and mitochondria; but the Z1A (KRT) allele clearly conferred a ~3-fold higher activity with DCA in GSTZ1 of both compartments.

Age is shown by the current study to be a major determinant of GSTZ1 expression and activity during human liver development. GSTZ1 was present at undetectable to very low levels in the fetal liver. Following birth, GSTZ1 level rose rapidly and reached nearly half of that of adults by one month of age. The increase continued until adolescence when GSTZ1 reached a stable level and maintained so throughout adulthood. The developmental change in GSTZ1 activity with DCA paralleled that of its protein expression. Therefore, the age-related increase in DCA-metabolizing activity did not explain the age-dependent decrease in DCA clearance observed in vivo after chronic treatment.

GSTZ1 haplotype had no effect on protein expression but did affect enzymatic activity with DCA. Z1A carriers possessed higher DCA-metabolizing activity than carriers of other alleles (Z1B, Z1C and Z1D) that had similar activity and expression. Accordingly, Z1A carriers exhibited a major impact in GSTZ1 activity in populations of older children and adults. The higher activity conferred by the Z1A allele was consistent to the generally faster clearance of DCA in its carriers after the 1st dose of 25 mg/kg DCA; however, this did not explain the greater reduction in plasma clearance after the 5th DCA dose as observed in Z1A/Z1A and Z1A/Z1D individuals. We speculate a haplotype-dependent susceptibility to DCA inactivation may exist and thus contribute to the in vivo differences after repeated doses.

Study of GSTZ1 inactivation using liver cytosol revealed that chloride attenuated DCA-induced inactivation of GSTZ1 in a chloride concentration- and GSTZ1 haplotype-dependent manner. In the absence of chloride, DCA rapidly reduced GSTZ1 activity to 50% of control level within 30 min for all individuals. At a physiological concentration of chloride in the liver (38 mM), cytosolic GSTZ1 inactivation $t_{1/2}$s were prolonged to 2.5 h for 1C/1A individuals and over 5 h for 1C and 1D homozygous individuals. In addition to chloride, other anions such as bromide, iodide and sulfite, were shown to protect GSTZ1 from DCA inactivation at 38 mM. The current finding of faster inactivation of GSTZ1 carrying the Z1A allele may explain at least in part the more marked reduction in DCA clearance after repeated doses in 1A/1A and 1A/1D individuals, compared with those carrying other haplotypes.

LIST OF REFERENCES

Alnouti Y and Klaassen CD (2008) Tissue distribution, ontogeny, and regulation of aldehyde dehydrogenase (Aldh) enzymes mRNA by prototypical microsomal enzyme inducers in mice. *Toxicol Sci* **101:**51-64.

Ammini CV, Fernandez-Canon J, Shroads AL, Cornett R, Cheung J, James MO, Henderson GN, Grompe M and Stacpoole PW (2003) Pharmacologic or genetic ablation of maleylacetoacetate isomerase increases levels of toxic tyrosine catabolites in rodents. *Biochem Pharmacol* **66:**2029-2038.

Anderson WB, Board PG and Anders MW (2004) Glutathione transferase zeta-catalyzed bioactivation of dichloroacetic acid: reaction of glyoxylate with amino acid nucleophiles. *Chem Res Toxicol* **17:**650-662.

Anderson WB, Board PG, Gargano B and Anders MW (1999) Inactivation of glutathione transferase zeta by dichloroacetic acid and other fluorine-lacking alpha-haloalkanoic acids. *Chem Res Toxicol* **12:**1144-1149.

Anderson WB, Liebler DC, Board PG and Anders MW (2002) Mass spectral characterization of dichloroacetic acid-modified human glutathione transferase zeta. *Chem Res Toxicol* **15:**1387-1397.

Andersson SM, Raiha NC and Ohisalo JJ (1980) Tyrosine aminotransferase activity in human fetal liver. *J Dev Physiol* **2:**17-27.

Archer SL, Gomberg-Maitland M, Maitland ML, Rich S, Garcia JG and Weir EK (2008) Mitochondrial metabolism, redox signaling, and fusion: a mitochondria-ROS-HIF-1alpha-Kv1.5 O2-sensing pathway at the intersection of pulmonary hypertension and cancer. *Am J Physiol Heart Circ Physiol* **294:**H570-578.

Barshop BA, Naviaux RK, McGowan KA, Levine F, Nyhan WL, Loupis-Geller A and Haas RH (2004) Chronic treatment of mitochondrial disease patients with dichloroacetate. *Molecular Genetics and Metabolism* **83:**138-149.

Berendzen K, Theriaque DW, Shuster J and Stacpoole PW (2006) Therapeutic potential of dichloroacetate for pyruvate dehydrogenase complex deficiency. *Mitochondrion* **6:**126-135.

Blackburn AC, Coggan M, Tzeng HF, Lantum H, Polekhina G, Parker MW, Anders MW and Board PG (2001) GSTZ1d: a new allele of glutathione transferase zeta and maleylacetoacetate isomerase. *Pharmacogenetics* **11:**671-678.

Blackburn AC, Tzeng HF, Anders MW and Board PG (2000) Discovery of a functional polymorphism in human glutathione transferase zeta by expressed sequence tag database analysis. *Pharmacogenetics* **10:**49-57.

Blackburn AC, Woollatt E, Sutherland GR and Board PG (1998) Characterization and chromosome location of the gene GSTZ1 encoding the human Zeta class glutathione transferase and maleylacetoacetate isomerase. *Cytogenet Cell Genet* **83:**109-114.

Board PG and Anders MW (2005) Human glutathione transferase zeta. *Methods Enzymol* **401:**61-77.

Board PG, Baker RT, Chelvanayagam G and Jermiin LS (1997) Zeta, a novel class of glutathione transferases in a range of species from plants to humans. *Biochem J* **328 (Pt 3):**929-935.

Board PG, Taylor MC, Coggan M, Parker MW, Lantum HB and Anders MW (2003) Clarification of the role of key active site residues of glutathione transferase zeta/maleylacetoacetate isomerase by a new spectrophotometric technique. *Biochem J* **374:**731-737.

Bull RJ (2000) Mode of action of liver tumor induction by trichloroethylene and its metabolites, trichloroacetate and dichloroacetate. *Environ Health Perspect* **108 Suppl 2:**241-259.

Calcutt NA, Lopez VL, Bautista AD, Mizisin LM, Torres BR, Shroads AL, Mizisin AP and Stacpoole PW (2009) Peripheral neuropathy in rats exposed to dichloroacetate. *J Neuropathol Exp Neurol* **68:**985-993.

Choudhary S, Xiao T, Vergara LA, Srivastava S, Nees D, Piatigorsky J and Ansari NH (2005) Role of aldehyde dehydrogenase isozymes in the defense of rat lens and human lens epithelial cells against oxidative stress. *Invest Ophthalmol Vis Sci* **46:**259-267.

Cornett R, James MO, Henderson GN, Cheung J, Shroads AL and Stacpoole PW (1999) Inhibition of glutathione S-transferase zeta and tyrosine metabolism by dichloroacetate: a potential unifying mechanism for its altered biotransformation and toxicity. *Biochem Biophys Res Commun* **262:**752-756.

Cui JY, Choudhuri S, Knight TR and Klaassen CD (2010) Genetic and epigenetic regulation and expression signatures of glutathione S-transferases in developing mouse liver. *Toxicol Sci* **116:**32-43.

Curry SH, Lorenz A, Chu PI, Limacher M and Stacpoole PW (1991) Disposition and pharmacodynamics of dichloroacetate (DCA) and oxalate following oral DCA doses. *Biopharm Drug Dispos* **12:**375-390.

De Koninck Y (2007) Altered chloride homeostasis in neurological disorders: a new target. *Curr Opin Pharmacol* **7:**93-99.

Delvalle JA and Greengard O (1977) Phenylalanine hydroxylase and tyrosine aminotransferase in human fetal and adult liver. *Pediatr Res* **11:**2-5.

Economopoulos KP and Sergentanis TN (2010) GSTM1, GSTT1, GSTP1, GSTA1 and colorectal cancer risk: A comprehensive meta-analysis. *European Journal of Cancer* **46:**1617-1631.

Edwards JC and Kahl CR (2010) Chloride channels of intracellular membranes. *FEBS Lett* **584:**2102-2111.

Fang YY, Kashkarov U, Anders MW and Board PG (2006) Polymorphisms in the human glutathione transferase zeta promoter. *Pharmacogenet Genomics* **16:**307-313.

Felitsyn N, McLeod C, Shroads AL, Stacpoole PW and Notterpek L (2008) The heme precursor delta-aminolevulinate blocks peripheral myelin formation. *Journal of Neurochemistry* **106:**2068-2079.

Fernandez-Canon JM, Baetscher MW, Finegold M, Burlingame T, Gibson KM and Grompe M (2002) Maleylacetoacetate isomerase (MAAI/GSTZ)-deficient mice reveal a glutathione-dependent nonenzymatic bypass in tyrosine catabolism. *Mol Cell Biol* **22:**4943-4951.

Fernandez-Canon JM and Penalva MA (1998) Characterization of a fungal maleylacetoacetate isomerase gene and identification of its human homologue. *J Biol Chem* **273:**329-337.

Fleischer S, McIntyre JO and Vidal JC (1979) Large-scale preparation of rat liver mitochondria in high yield. *Methods Enzymol* **55:**32-39.

Forner F, Foster LJ, Campanaro S, Valle G and Mann M (2006) Quantitative proteomic comparison of rat mitochondria from muscle, heart, and liver. *Mol Cell Proteomics* **5:**608-619.

Fulda S, Galluzzi L and Kroemer G (2010) Targeting mitochondria for cancer therapy. *Nat Rev Drug Discov* **9:**447-464.

Gallagher EP, Gardner JL and Barber DS (2006) Several glutathione S-transferase isozymes that protect against oxidative injury are expressed in human liver mitochondria. *Biochem Pharmacol* **71:**1619-1628.

Garcia-Espana A, Alonso E and Rubio V (1991) Influence of anions on the activation of carbamoyl phosphate synthetase (ammonia) by acetylglutamate: implications for the activation of the enzyme in the mitochondria. *Arch Biochem Biophys* **288:**414-420.

Goto S, Kawakatsu M, Izumi S-i, Urata Y, Kageyama K, Ihara Y, Koji T and Kondo T (2009) Glutathione S-transferase π localizes in mitochondria and protects against oxidative stress. *Free Radic Biol Med* **46:**1392-1403.

Guo X, Dixit V, Liu H, Shroads AL, Henderson GN, James MO and Stacpoole PW (2006) Inhibition and recovery of rat hepatic glutathione S-transferase zeta and

alteration of tyrosine metabolism following dichloroacetate exposure and withdrawal. *Drug Metab Dispos* **34:**36-42.

Hansen JM, Go YM and Jones DP (2006) Nuclear and mitochondrial compartmentation of oxidative stress and redox signaling. *Annu Rev Pharmacol Toxicol* **46:**215-234.

Hassoun EA, Cearfoss J and Spildener J (2010) Dichloroacetate- and trichloroacetate-induced oxidative stress in the hepatic tissues of mice after long-term exposure. *J Appl Toxicol* **30:**450-456.

Hayes JD, Flanagan JU and Jowsey IR (2005) Glutathione transferases. *Annu Rev Pharmacol Toxicol* **45:**51-88.

Henderson GN, Yan Z, James MO, Davydova N and Stacpoole PW (1997) Kinetics and metabolism of chloral hydrate in children: identification of dichloroacetate as a metabolite. *Biochem Biophys Res Commun* **235:**695-698.

Hines RN (2008) The ontogeny of drug metabolism enzymes and implications for adverse drug events. *Pharmacology & Therapeutics* **118:**250-267.

Hines RN, Koukouritaki SB, Poch MT and Stephens MC (2008) Regulatory polymorphisms and their contribution to interindividual differences in the expression of enzymes influencing drug and toxicant disposition. *Drug Metab Rev* **40:**263-301.

James MO, Cornett R, Yan Z, Henderson GN and Stacpoole PW (1997) Glutathione-dependent conversion to glyoxylate, a major pathway of dichloroacetate biotransformation in hepatic cytosol from humans and rats, is reduced in dichloroacetate-treated rats. *Drug Metab Dispos* **25:**1223-1227.

James MO, Fouts JR and Bend JR (1976) Hepatic and extrahepatic metabolism, *in vitro*, of an epoxide (8-^{14}C-styrene oxide) in the rabbit. *Biochem Pharmacol* **25:**187-193.

James MO, Yan Z, Cornett R, Jayanti VMKM, Henderson GN, Davydova N, Katovich MJ, Pollock B and Stacpoole PW (1998) Pharmacokinetics and metabolism of [^{14}C]dichloroacetate in male Sprague-Dawley rats. Identification of glycine conjugates, including hippurate, as urinary metabolites of dichloroacetate. *Drug Metab Dispos* **26:**1134-1143.

Kaufmann P, Engelstad K, Wei Y, Jhung S, Sano MC, Shungu DC, Millar WS, Hong X, Gooch CL, Mao X, Pascual JM, Hirano M, Stacpoole PW, DiMauro S and De Vivo DC (2006) Dichloroacetate causes toxic neuropathy in MELAS: A randomized, controlled clinical trial. *Neurology* **66:**324-330.

Keller A, Nesvizhskii AI, Kolker E and Aebersold R (2002) Empirical statistical model to estimate the accuracy of peptide identifications made by MS/MS and database search. *Anal Chem* **74:**5383-5392.

Kitani T and Fujisawa H (1984) Influence of salts on the activity and the subunit structure of ornithine decarboxylase from rat liver. *Biochim Biophys Acta* **784:**164-167.

Koukouritaki SB, Simpson P, Yeung CK, Rettie AE and Hines RN (2002) Human hepatic flavin-containing monooxygenases 1 (FMO1) and 3 (FMO3) developmental expression. *Pediatr Res* **51:**236-243.

Langaee T and Ronaghi M (2005) Genetic variation analyses by Pyrosequencing. *Mutat Res* **573:**96-102.

Lantum HB, Baggs RB, Krenitsky DM, Board PG and Anders MW (2002a) Immunohistochemical localization and activity of glutathione transferase zeta (GSTZ1-1) in rat tissues. *Drug Metab Dispos* **30:**616-625.

Lantum HB, Cornejo J, Pierce RH and Anders MW (2003) Perturbation of maleylacetoacetic acid metabolism in rats with dichloroacetic Acid-induced glutathione transferase zeta deficiency. *Toxicol Sci* **74:**192-202.

Lantum HB, Liebler DC, Board PG and Anders MW (2002b) Alkylation and inactivation of human glutathione transferase zeta (hGSTZ1-1) by maleylacetone and fumarylacetone. *Chem Res Toxicol* **15:**707-716.

Larson JL and Bull RJ (1992) Metabolism and lipoperoxidative activity of trichloroacetate and dichloroacetate in rats and mice. *Toxicol Appl Pharmacol* **115:**268-277.

Leonard MO, Kieran NE, Howell K, Burne MJ, Varadarajan R, Dhakshinamoorthy S, Porter AG, O'Farrelly C, Rabb H and Taylor CT (2006) Reoxygenation-specific activation of the antioxidant transcription factor Nrf2 mediates cytoprotective gene expression in ischemia-reperfusion injury. *Faseb J* **20:**2624-2626.

Lin EL, Mattox JK and Daniel FB (1993) Tissue distribution, excretion, and urinary metabolites of dichloroacetic acid in the male Fischer 344 rat. *J Toxicol Environ Health* **38:**19-32.

Mannervik B, Board PG, Hayes JD, Listowsky I and Pearson WR (2005) Nomenclature for mammalian soluble glutathione transferases. *Methods Enzymol* **401:**1-8.

McMurtry MS, Bonnet S, Wu X, Dyck JRB, Haromy A, Hashimoto K and Michelakis ED (2004) Dichloroacetate Prevents and Reverses Pulmonary Hypertension by Inducing Pulmonary Artery Smooth Muscle Cell Apoptosis. *Circ Res* **95:**830-840.

Meijer AJ, Baquet A, Gustafson L, van Woerkom GM and Hue L (1992) Mechanism of activation of liver glycogen synthase by swelling. *J Biol Chem* **267:**5823-5828.

Michelakis ED, Webster L and Mackey JR (2008) Dichloroacetate (DCA) as a potential metabolic-targeting therapy for cancer. *Br J Cancer* **99:**989-994.

Mitsuhashi H, Ikeuchi H, Yamashita S, Kuroiwa T, Kaneko Y, Hiromura K, Ueki K and Nojima Y (2004) Increased levels of serum sulfite in patients with acute pneumonia. *Shock* **21:**99-102.

Monster AC (1986) Biological monitoring of chlorinated hydrocarbon solvents. *J Occup Med* **28:**583-588.

Mootha VK, Bunkenborg J, Olsen JV, Hjerrild M, Wisniewski JR, Stahl E, Bolouri MS, Ray HN, Sihag S, Kamal M, Patterson N, Lander ES and Mann M (2003) Integrated analysis of protein composition, tissue diversity, and gene regulation in mouse mitochondria. *Cell* **115:**629-640.

Morrison G (1990) Serum Chloride, in: *Clinical methods: the history, physical, and laboratory examinations. 3rd edition.* (Walker HK, Hall WD and Hurst JW eds), Butterworths, Boston.

Mughal FH (1992) Chlorination of drinking water and cancer: a review. *J Environ Pathol Toxicol Oncol* **11:**287-292.

Nesvizhskii AI, Keller A, Kolker E and Aebersold R (2003) A statistical model for identifying proteins by tandem mass spectrometry. *Anal Chem* **75:**4646-4658.

Ohisalo JJ, Laskowska-Klita T and Andersson SM (1982) Development of tyrosine aminotransferase and para-hydroxyphenylpyruvate dioxygenase activities in fetal and neonatal human liver. *J Clin Invest* **70:**198-200.

Pallotti F and Lenaz G (2007) Isolation and subfractionation of mitochondria from animal cells and tissue culture lines. *Methods Cell Biol* **80:**3-44.

Pfanner N and Geissler A (2001) Versatility of the mitochondrial protein import machinery. *Nat Rev Mol Cell Biol* **2:**339-349.

Polekhina G, Board PG, Blackburn AC and Parker MW (2001) Crystal structure of maleylacetoacetate isomerase/glutathione transferase zeta reveals the molecular basis for its remarkable catalytic promiscuity. *Biochemistry* **40:**1567-1576.

Raza H, Robin M-A, Fang J-K and Avadhani NG (2002) Multiple isoforms of mitochondrial glutathione S-transferases and their differential induction under oxidative stress. *Biochem J* **366:**45-55.

Ricci G, Turella P, De Maria F, Antonini G, Nardocci L, Board PG, Parker MW, Carbonelli MG, Federici G and Caccuri AM (2004) Binding and kinetic

mechanisms of the Zeta class glutathione transferase. *J Biol Chem* **279:**33336-33342.

Robin MA, Prabu SK, Raza H, Anandatheerthavarada HK and Avadhani NG (2003) Phosphorylation enhances mitochondrial targeting of GSTA4-4 through increased affinity for binding to cytoplasmic Hsp70. *J Biol Chem* **278:**18960-18970.

Russo PA, Mitchell GA and Tanguay RM (2001) Tyrosinemia: a review. *Pediatr Dev Pathol* **4:**212-221.

Sasaki T, Aizawa T, Kamiya M, Kikukawa T, Kawano K, Kamo N and Demura M (2009) Effect of chloride binding on the thermal trimer-monomer conversion of halorhodopsin in the solubilized system. *Biochemistry* **48:**12089-12095.

Sharma V and Schwille PO (1993) Sulfite inhibits oxalate production from glycolate and glyoxylate in vitro and from dichloroacetate infused i.v. into male rats. *Biochem Med Metab Biol* **49:**265-269.

Sheffield J, Taylor N, Fauquet C and Chen S (2006) The cassava (Manihot esculenta Crantz) root proteome: protein identification and differential expression. *Proteomics* **6:**1588-1598.

Shroads AL, Guo X, Dixit V, Liu HP, James MO and Stacpoole PW (2008) Age-dependent kinetics and metabolism of dichloroacetate: possible relevance to toxicity. *J Pharmacol Exp Ther* **324:**1163-1171.

Shroads AL, Langaee T, Coats BS, Kurtz TL, Bullock JR, Weithorn D, Gong Y, Wagner DA, Ostrov DA, Johnson JA and Stacpoole PW (2011) Human Polymorphisms in the Glutathione Transferase Zeta 1/Maleylacetoacetate Isomerase Gene Influence the Toxicokinetics of Dichloroacetate. *The Journal of Clinical Pharmacology***:**(Accepted).

Stacpoole PW (1969) Review of the pharmacologic and therapeutic effects of diisopropylammonium dichloroacetate (DIPA). *J Clin Pharmacol J New Drugs* **9:**282-291.

Stacpoole PW (1989) The pharmacology of dichloroacetate. *Metabolism* **38:**1124-1144.

Stacpoole PW (2011) The Dichloroacetate Dilemma: Environmental Hazard vs. Therapeutic Goldmine - Both or Neither? *Environ Health Perspect* **119:**155-158.

Stacpoole PW, Gilbert LR, Neiberger RE, Carney PR, Valenstein E, Theriaque DW and Shuster JJ (2008) Evaluation of long-term treatment of children with congenital lactic acidosis with dichloroacetate. *Pediatrics* **121:**e1223-1228.

Stacpoole PW, Henderson GN, Yan Z, Cornett R and James MO (1998) Pharmacokinetics, metabolism, and toxicology of dichloroacetate. *Drug Metab Rev* **30:**499 - 539.

Stacpoole PW, Kerr DS, Barnes C, Bunch ST, Carney PR, Fennell EM, Felitsyn NM, Gilmore RL, Greer M, Henderson GN, Hutson AD, Neiberger RE, O'Brien RG, Perkins LA, Quisling RG, Shroads AL, Shuster JJ, Silverstein JH, Theriaque DW and Valenstein E (2006) Controlled Clinical Trial of Dichloroacetate for Treatment of Congenital Lactic Acidosis in Children. *Pediatrics* **117:**1519-1531.

Stacpoole PW, Nagaraja NV and Hutson AD (2003) Efficacy of dichloroacetate as a lactate-lowering drug. *J Clin Pharmacol* **43:**683-691.

Stephens M, Smith NJ and Donnelly P (2001) A new statistical method for haplotype reconstruction from population data. *Am J Hum Genet* **68:**978-989.

Strange RC, Howie AF, Hume R, Matharoo B, Bell J, Hiley C, Jones P and Beckett GJ (1989) The development expression of alpha-, mu- and pi-class glutathione S-transferases in human liver. *Biochim Biophys Acta* **993:**186-190.

Tavoulari S, Forrest LR and Rudnick G (2009) Fluoxetine (Prozac) binding to serotonin transporter is modulated by chloride and conformational changes. *J Neurosci* **29:**9635-9643.

Theodoratos A, Tu WJ, Cappello J, Blackburn AC, Matthaei K and Board PG (2009) Phenylalanine-induced leucopenia in genetic and dichloroacetic acid generated deficiency of glutathione transferase Zeta. *Biochemical Pharmacology* **77:**1358-1363.

Tong Z, Board PG and Anders MW (1998a) Glutathione transferase zeta-catalyzed biotransformation of dichloroacetic acid and other alpha-haloacids. *Chem Res Toxicol* **11:**1332-1338.

Tong Z, Board PG and Anders MW (1998b) Glutathione transferase zeta catalyses the oxygenation of the carcinogen dichloroacetic acid to glyoxylic acid. *Biochem J* **331(Pt 2):**371-374.

Tzeng HF, Blackburn AC, Board PG and Anders MW (2000) Polymorphism- and species-dependent inactivation of glutathione transferase zeta by dichloroacetate. *Chem Res Toxicol* **13:**231-236.

WHO (2004) Dichloroacetic Acid (IARC Monographs on the Evaluation of Carcinogenic Risks to Humans, Volume 84).

WHO (2005) Dichloroacetic Acid in Drinking-water.

Widdowson EM and Dickerson JW (1960) The effect of growth and function on the chemical composition of soft tissues. *Biochem J* **77:**30-43.

Zhang T, Wu Q, Sun HW, Rao J and Kannan K (2010) Perchlorate and iodide in whole blood samples from infants, children, and adults in Nanchang, China. *Environ Sci Technol* **44:**6947-6953.

BIOGRAPHICAL SKETCH

Wenjun Li was born in 1984 in Guangzhou, China, being the only child of Jianguo Li and Xiangling Jian. She spent the first 18 years with her parents living in Shenzhen, a young and vigorous city that she loves so much and cherishes some of her best memories with. After graduation from Shenzhen Experimental School in 2002, she was admitted to Sun Yat-sen University, spending the first two years in beautiful Zhuhai Campus and the latter two years in the historical Medical Campus in Guangzhou. She wanted to study medicine but was eventually accepted to major in pharmaceutical sciences. During undergraduate, she enjoyed learning chemistry but found herself more apt in doing biological experiments. The desire to combine the knowledge of chemistry to the practice of biology inspired and eventually motivated her to pursue her doctoral degree in the Department of Medicinal Chemistry, University of Florida in 2006. After graduation, she wishes to obtain a postdoctoral training in Europe. Her goal is to establish a professional career in biomedical research and step on the soil of as many countries as she can.